termination to epitope peptides of omega-5 gliadin and high molecular weight glutenin subunit is a useful tool for diagnosis of wheat-dependent exercise-induced anaphylaxis. *J Immunol* 2005;**175**:8116-22.
26. Sampson HA. Utility of food-specific IgE concentrations in predicting symptomatic food allergy. *J Allergy Clin Immunol* 2001;**107**:891-6.
27. Komata T, Söderström L, Borres MP, Tachimoto H, Ebisawa M. The predictive relationship of food-specific serum IgE concentrations to challenge outcomes for egg and milk varies by patient age. *J Allergy Clin Immunol* 2007;**119**:1272-4.
28. Lorenz AR, Schuerer S, Haustein D, Vieths S. Recombinant food allergens. *J Chromatogr B Biomed Sci Appl* 2001;**756**:255-79.
29. Bohle B, Vieths S. Improving diagnostic tests for food allergy with recombinant allergens. *Methods* 2004;**32**:292-9.
30. Matsuo H, Kohno K, Morita E. Molecular cloning, recombinant expression and IgE-binding epitope of omega-5 gliadin, a major allergen in wheat-dependent exercise-induced anaphylaxis. *FEBS J* 2005;**272**:4431-8.
31. Matsuo H, Dahlström J, Tanaka A *et al.* Sensitivity and specificity of recombinant omega-5 gliadin-specific IgE measurement for the diagnosis of wheat-dependent exercise-induced anaphylaxis. *Allergy* 2008;**63**:233-6.
32. Takahashi H, Tanaka A, Dahlström J, Kohno K, Matsuo H, Morita E. Utilization of the recombinant HMW-glutenin for diagnosis of wheat-dependent exercise-induced anaphylaxis [abstract]. *Allergy* 2007;**62** (Suppl 83):370.
33. Jacquenet S, Morisset M, Battais F *et al.* Interest of ImmunoCAP system to recombinant omega-5 gliadin for the diagnosis of exercise-induced wheat allergy. *Int Arch Allergy Immunol* 2008;**149**:74-80.
34. Ito K, Futamura M, Borres MP *et al.* IgE antibodies to omega-5 gliadin associate with immediate symptoms on oral wheat challenge in Japanese children. *Allergy* 2008; **63**:1536-42.
35. Beyer K, Chung D, Schulz G *et al.* The role of wheat omega-5 gliadin IgE antibodies as a diagnostic tool for wheat allergy in childhood. *J Allergy Clin Immunol* 2008; **122**:419-21.
36. Katsunuma T, Iikura Y, Akasawa A, Iwasaki A, Hashimoto K, Akimoto K. Wheat-dependent exercise-induced anaphylaxis: inhibition by sodium bicarbonate. *Ann Allergy* 1992;**68**:184-8.
37. Matsuo H, Morimoto K, Akaki T *et al.* Exercise and aspirin increase levels of circulating gliadin peptides in patients with wheat-dependent exercise-induced anaphylaxis. *Clin Exp Allergy* 2005;**35**:461-6.
38. Harada S, Horikawa T, Ashida M, Kamo T, Nishioka E, Ichihashi M. Aspirin enhances the induction of type I allergic symptoms when combined with food and exercise in patients with food-dependent exercise-induced anaphylaxis. *Br J Dermatol* 2001;**145**:336-9.
39. Aihara M, Miyazawa M, Osuna H *et al.* Food-dependent exercise-induced anaphylaxis: influence of concurrent aspirin administration on skin testing and provocation. *Br J Dermatol* 2002;**146**:466-72.
40. Fujii H, Kambe N, Fujisawa A, Kohno K, Morita E, Miyachi Y. Food-dependent exercise-induced anaphylaxis induced by low dose aspirin therapy. *Allergol Int* 2008;**57**: 97-8.
41. Matsuo H, Kaneko S, Tsujino Y *et al.* Effects of nonsteroidal anti-inflammatory drugs (NSAIDs) on serum allergen levels after wheat ingestion. *J Dermatol Sci* 2009; **53**:241-3. Epub 2008 Oct 22.
42. Harada S, Horikawa T, Ichihashi M. [A study of food-dependent exercise-induced anaphylaxis by analyzing the Japanese cases reported in the literature]. *Arerugi [Jpn J Allergol]* 2000;**49**:1066-73 (in Japanese).

The American Journal of Pathology, Vol. 176, No. 2, February 2010
Copyright © American Society for Investigative Pathology
DOI: 10.2353/ajpath.2010.090454

Epithelial and Mesenchymal Cell Biology

Involvement of Wnt Signaling in Dermal Fibroblasts

Kenji Kabashima,*†‡ Jun-ichi Sakabe,* Ryutaro Yoshiki,* Yasuhiko Tabata,§ Kimitoshi Kohno,¶ and Yoshiki Tokura*

From the Departments of Dermatology and Molecular Biology,¶ School of Medicine, University of Occupational and Environmental Health, Kitakyushu; the Department of Dermatology,† and Center for Innovation in Immunoregulative Technology and Therapeutics,‡ Kyoto University Graduate School of Medicine, Kyoto; and the Institute for Frontier Medical Sciences,§ Kyoto University, Kyoto, Japan*

Pachydermoperiostosis (PDP) is a rare disease characterized by unique phenotypes of the skin and bone, such as thick skin, implying that it may be caused by dysregulation of mesenchymal cells. The aim of this study is to examine the roles of dermal fibroblasts in the pathogenesis of pachydermia in association with Wnt signaling. The numbers of cultured fibroblasts were compared between healthy donors and PDP patients, and mRNA expression profiles in cultured dermal fibroblasts were examined by DNA microarray analysis and real-time reverse transcription-PCR. DKK1 and β-catenin protein expressions were also evaluated by immunohistochemistry in the skin. To evaluate the *in vivo* roles of DKK1 in mice, *DKK1* small interfering RNA was injected to the ears. We found that PDP fibroblasts proliferated more than control fibroblasts and that mRNA expression of a Wnt signaling antagonist, *DKK1*, was much lower in PDP fibroblasts than in normal ones. Consistently, decreased expression of DKK1 in fibroblasts and enhanced expression of β-catenin were noted in PDP patients. Moreover, recombinant human DKK1 protein decreased the proliferation of dermal fibroblasts. In accord with the above human studies, intradermal injections of *DKK1* small interfering RNA into mouse ears increased ear thickness as seen in PDP. Our findings suggest that enhanced Wnt signaling contributes to the development of pachydermia by enhancing dermal fibroblast functions. *(Am J Pathol 2010, 176:721–732; DOI: 10.2353/ajpath.2010.090454)*

Pachydermoperiostosis (PDP), a form of primary hypertrophic osteoarthropathy, is a rare disease[1–3] diagnosed by the presence of a triad of pachydermia (skin thickening), digital clubbing, and periostosis of long bones. Typically, insidious development of thickening of the fingers and toes, clubbing of the terminal phalanges, enlargement of the hands and feet, hyperhidrosis, increased sebaceous secretion, and velvet coloration of the skin occur mostly in men during adolescence.[4] Radiographic signs of bilateral and symmetrical periostosis are frequently observed as a marked irregular periosteal ossification of the tibias and fibulas.[3] Touraine et al[5] recognized PDP with three clinical presentations or forms: a "complete form" presenting the full-blown phenotype; an "incomplete form" characterized by the phenotype without pachydermia; and a "fruste form" with pachydermia and minimal or absent skeletal changes.

Recently, the incomplete form of PDP, primary osteoarthropathy without pachydermia, was mapped to chromosome 4q33-q34, and gene mutations in *HPGD*, encoding 15-hydroxyprostaglandin dehydrogenase, the main enzyme of prostaglandin (PG) degradation, were identified.[6] Therefore, it has been suggested that the digital clubbing and bone changes are due to elevated PGE_2. However, the pathomechanism underlying pachydermia of PDP remains unknown.

Since the major manifestations of complete PDP occur in both skin and bone, the etiology could be related to the dysregulation of bone morphogenetic proteins (BMP), transforming growth factor (TGF)-β, and/or wingless (Wnt) pathways.[7–9] The Wnt signaling consists of canonical and non-canonical pathways. The canonical pathway involves cytosolic β-catenin stabilization, nuclear translocation and gene regulation, and the non-canonical pathways activate rho, rac, JNK, and protein kinase C.[10,11] These signaling pathways are mediated by Wnt protein, which binds to a frizzled Wnt receptor. Wnt signaling is modulated by several different families of

Supported in part by grants from the Ministry of Education, Culture, Sports, Science and Technology and the Ministry of Health, Labour and Welfare of Japan.

K.K. and J.S. contributed equally to this work.

Accepted for publication October 20, 2009.

Address reprint requests to Dr. Kenji Kabashima, Department of Dermatology, Kyoto University Graduate School of Medicine, 54 Shogoin Kawaracho, Sakyo-ku, Kyoto 606-8507, Japan. E-mail: kaba@kuhp.kyoto-u.ac.jp.

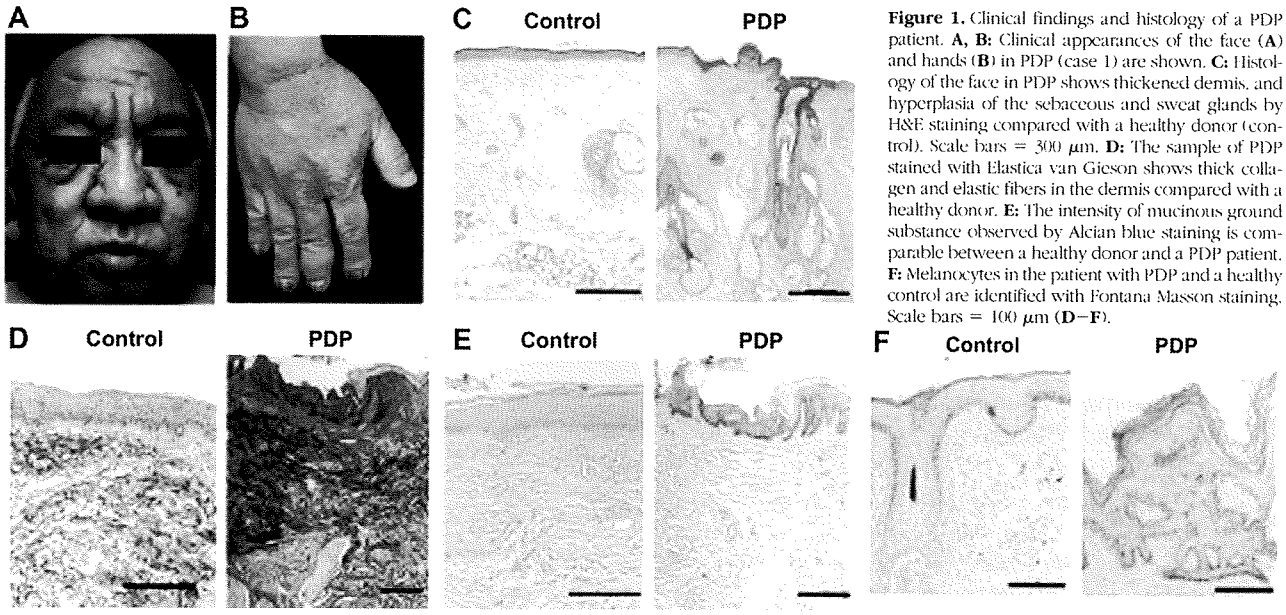

Figure 1. Clinical findings and histology of a PDP patient. **A, B:** Clinical appearances of the face (**A**) and hands (**B**) in PDP (case 1) are shown. **C:** Histology of the face in PDP shows thickened dermis, and hyperplasia of the sebaceous and sweat glands by H&E staining compared with a healthy donor (control). Scale bars = 300 μm. **D:** The sample of PDP stained with Elastica van Gieson shows thick collagen and elastic fibers in the dermis compared with a healthy donor. **E:** The intensity of mucinous ground substance observed by Alcian blue staining is comparable between a healthy donor and a PDP patient. **F:** Melanocytes in the patient with PDP and a healthy control are identified with Fontana Masson staining. Scale bars = 100 μm (**D**–**F**).

secreted down-regulators. Among them, Dickkopf (DKK) is a family of cysteine-rich proteins comprising at least four different forms (DKK1, DKK2, DKK3, and DKK4), which are coordinately expressed in mesodermal lineages. The best studied of these is DKK1, which blocks the canonical Wnt signaling by inducing endocytosis of lipoprotein receptor-related protein 5/6 (LRP5/6) complex[12] without affecting the frizzled Wnt receptor.[13] DKK1 induces the formation of ectopic heads in *Xenopus laevis* in the presence of BMP inhibitors[14] and modulates apoptosis during vertebrate limb development.[15] High mRNA levels of *DKK1* in human dermal fibroblasts of the palms and soles inhibit the function and proliferation of melanocytes via the suppression of β-catenin and microphthalmia-associated transcription factor.[16,17] In parallel, DKK1 transgenic mice under the control of keratin 14 have no pigmentation on the trunk because of the absence of melanocytes in the inner-follicular epidermis, as well as the lack of hair follicle development.[18] These findings suggest that DKK1 is deeply involved in the formation and differentiation of the skin.

Here we investigated two complete cases of PDP using dermal fibroblasts to address the pathogenetic mechanisms. DNA microarray analysis revealed that the proliferation of primary fibroblasts of PDP was increased with decreased expression of *DKK1* mRNA in cultured fibroblasts. Consistent with this finding, immunohistochemistry indicated decreased expression of DKK1 in fibroblasts and enhanced expression of β-catenin in the skin of patients with PDP, suggesting that Wnt signaling is enhanced in PDP. The intradermal injection of *DKK1* synthetic small interfering RNA (siRNA) increased the ear thickness of mice as seen in PDP. These results suggest that enhanced Wnt signaling contributes to the development of pachydermia.

Materials and Methods

Patients

Case 1

A 50-year-old male was referred to our clinic. The skin on his head and face was thick and oily with a dark velvet color. Naso-labial folds and transverse furrowing of the forehead were prominent (Figure 1A). The hands were enlarged with marked clubbing of the second and fifth digits, as compared with those of an age- and sex-matched healthy donor (Figure 1B). These symptoms developed when he was 18 years old. X-ray examination of the long bones showed major periostosis with cortical thickening and widening of the shafts (data not shown). Histology of the skin showed thickened dermis, and sebaceous and sweat gland enlargement, as compared with that of a healthy control (Figure 1C). Elastica van Gieson staining showed thick and interwoven collagen bundles in some areas of the dermis and also thick and partially fragmented elastic fibers in PDP (Figure 1D). The intensity of mucinous ground substance observed by Alcian blue staining was comparable between a healthy control and a PDP patient (Figure 1E). On the other hand, Fontana Masson staining revealed that the number of melanocytes and the intensity of the staining in the patient with PDP was higher than that in a healthy control (Figure 1F). Neither hepatosplenomegaly nor internal malignancy was found on physical examination or computed tomography scans. Biochemical tests showed normal levels of thyroid-stimulating hormone and growth hormone, which likely rules out thyroid acropathy and acromegaly. Family history was noncontributory. Based on these clinical manifestations and histological findings, the patient was diagnosed as the complete form of PDP.

Case 2

The patient was a 38-year-old male with clinical findings similar to case 1, including pachydermia, digital clubbing, and periostosis. He had no signs or symptoms of hepatosplenomegaly, pulmonary diseases, tumoral syndrome, thyroid acropathy, or acromegaly (data not shown) as reported previously.[19]

Cell Preparation, Culture, and Reagents

Skin biopsies of the right temple (case 1) and scalp (case 2) were performed for histology and primary culture of fibroblasts. Control donors were matched for age, sex, and biopsy site, and the samples were processed in parallel. Institutional approval and informed consent were obtained from all subjects. The biopsy samples were immersed in Dulbecco's Modified Eagle Medium (Sigma, St. Louis, MO) containing 10% heat-inactivated fetal calf serum (Invitrogen, Carlsbad, CA), 5×10^{-5} mol/L 2-mercaptoethanol, 2 mmol/L L-glutamine, 25 mmol/L HEPES (Cellgro, Herndon, VA), 1 mmol/L nonessential amino acids, 1 mmol/L sodium pyruvate, 100 units/ml penicillin, and 100 μg/ml streptomycin, with 5% CO_2 at 37°C. The fibroblasts were allowed to adhere to the surface of 100-mm plastic tissue culture dishes (Nunc, Roskilde, Denmark). To evaluate the number of fibroblasts, 2×10^5 third-passage fibroblasts were seeded in 1 ml of medium in 24-well dishes and resuspended with trypsin/EDTA 1 week later. The numbers of fibroblasts were evaluated 7 and 14 days after seeding by flow cytometry using FACSCanto (BD Biosciences, San Diego, CA) with standard beads Flow Count (Beckman Coulter, Fullerton, CA) as per the manufacturer's instructions. The actin bundle formation of cultured fibroblasts from a healthy individual and an individual with PDP were examined by staining with alexa 488-labeled phalloidin antibody (Invitrogen) 5 days after the fourth passage.

For treatment with DKK1, fibroblasts were harvested 5 days after a comparable number of passages and cultured again at 1×10^6 cells in one ml of medium with or without recombinant human DKK1 (R&D Systems Inc., Minneapolis, MN) for another 2 days. For treatment with PGE_2, fibroblasts were harvested 5 days after a comparable number of passages and cultured again at 1×10^5 cells in two ml of medium with or without PGE_2 (Sigma) in the presence of indomethacin (10 μmol/L; Cayman Chemical Co., Ann Arbor, MI) for another 4 days.

Flow Cytometry and Histology

Flow cytometric analysis was performed with doublet discrimination on the FACSCanto[20] and FlowJo software (TreeStar, San Carlos, CA).[21] Human fibroblasts were treated with cytofix/cytoperm buffer according to the manufacturer's protocol (BD Biosciences). For cell cycle analysis, fibroblasts were incubated with 7-amino actinomycin D (7-AAD) (BD Biosciences) for 20 minutes at 4°C. After staining with 7-AAD, the DNA contents were analyzed by flow cytometry. For β-catenin staining, fibroblasts were stained with phycoerythrin-labeled β-catenin antibody (H-102, Santa Cruz Biotechnology Inc., Santa Cruz, CA), and mean fluorescence intensity was evaluated by flow cytometry.

For histology, the biopsy samples and the ears of mice were fixed in 10% formaldehyde. Sections of 5-μm thickness were prepared and stained with H&E, Elastica van Gieson, or Alcian blue. Immunohistochemical staining on paraffin-embedded sections was performed using a Vectastain ABC kit (Vector Laboratories, Burlingame, CA).[20] Antibodies used were rabbit anti-human polyclonal DKK1 (ab61034, Abcam, Cambridge, UK), mouse monoclonal anti-human β-catenin IgG1 (610153, BD Biosciences, San Diego, CA), and rabbit anti-human polyclonal proliferating cellular nuclear antigen antibodies (SC-7907, Santa Cruz Biotechnology Inc., Santa Cruz, CA). The control antibodies used were rabbit non-immune serum or mouse IgG1 (X0931, Dako, Glostrup, Denmark). The immunoreactivity was visualized by Fast Red or diaminobenzidine (Sigma), and the sections were then counterstained with hematoxylin. Images were acquired on a 600CL-CU cooled charge-coupled device video camera (Pixera, Los Gatos, CA) and processed with InStudio 1.0.0 (Pixera).

Western Blot Analysis

For Western blotting studies, fibroblasts were isolated from a healthy donor. Cytoplasm- and nuclear- proteins were extracted by NucBuster Protein Extraction Kit (Novagen, Darmstadt, Germany). Twenty μg protein samples were electrophoresed by 8% SDS-polyacrylamide gel electrophoresis and electroblotted onto polyvinylidene difluoride membranes for 2 hours at 180 mA. After blocking with 5% skim milk solution, the membranes were incubated with rabbit anti-human β-catenin (SC-7199; 1:1000, Santa Cruz Biotechnology Inc.) polyclonal antibodies or rabbit anti-human glyceraldehyde-3-phosphate dehydrogenase (SC-25778; 1:1000, Santa Cruz Biotechnology Inc.) antibody and detected with horseradish peroxidase-conjugated goat anti-rabbit IgG (Bio-Rad, Hercules, CA). Immunoblots were visualized using the ECL Plus Western Blotting Detection Reagents (GE Health care, Buckinghamshire, UK) according to the manufacturer's protocol. Bands were quantified by densitometry with the help of a CS Analyzer ver. 2.0 (ATTO, Tokyo, Japan).

Quantitative Reverse Transcription-PCR and Microarray Procedures

Total RNA was extracted from three-passage fibroblasts (case 1 and the control) cultured for 2 days with the RNeasy Mini Kit (QIAGEN, Valencia, CA). cDNA was reverse transcribed from total RNA samples using the TaqMan Reverse Transcription (RT) reagents (Applied Biosystems, Foster City, CA). Human *DKK1* (Assay ID: Hs00183740) mRNA expression was quantified using TaqMan Gene Expression Assay (Applied Biosystems) with the ABI PRISM 7700 sequence detection system (Applied Biosystems). As an endogenous reference for these RT-PCR quantification studies, human *GAPDH* con-

Table 1. PCR and Sequencing Primers

PCR Primer	Sequence	Tm	Binding site
hDKK1-Exon1, 2			
Forward	5′-CGTCTGCTATAACGCTCGCTGGTAG-3′	77	Promoter
Reverse	5′-AATTCATAGACGCTCAAAGGCTGGA-3′	73	Intron2
hDKK1-Exon3, 4			
Forward	5′-ACTTGCCCCTACCACAGTTG-3′	70	Intron2
Reverse	5′-GTTCCTGCCAATCACCAAGT-3′	68	3′UTR
hTCF-4-Exon1			
Forward	5′-TGGCTTTTCTTCCTCCTTCA-3′	66	5′UTR
Reverse	5′-AGAAAAAGAATCGGCGAGGT-3′	66	Intron1
hTCF-4-6			
Forward	5′-GCGATTTCTGGCAGGTAGTC-3′	70	Intron7
Reverse	5′-TAGCGATCCAGGAAGATGCT-3′	68	Intron10
hTCF-4-9			
Forward	5′-TTAGTAGGGGTTGGGGGAAG-3′	70	Intron13
Reverse	5′-TTGGTAGAATCATGAGGTTCTTCTC-3′	71	3′UTR
hHPGD Exon1			
Forward	5′-GCTGGCTTGACAGTTTCCTC-3′	70	5′UTR
Reverse	5′-CAGCCTCAGCTTCAGCAAAT-3′	68	Intron1
hHPGD Exon2			
Forward	5′-TTGCTGAAGCTGAGGCTGT-3′	68	Intron1
Reverse	5′-TCTTGCCTTTCTTTCGGTTT-3′	64	Intron2
hHPGD Exon3			
Forward	5′-TCCACAAACCACACATTGAGA-3′	67	Intron2
Reverse	5′-CCAGCTTTCTGTAACTTCCCTTT-3′	70	Intron3
hHPGD Exon4			
Forward	5′-TAGGCAAACCCAAAGAATCC-3′	66	Intron3
Reverse	5′-CACATGGGAGCAGAGACATC-3′	70	Intron4
hHPGD Exon5			
Forward	5′-CCTGGGGAGGCAGAAAAA-3′	67	Intron4
Reverse	5′-TTTATTTGGTTCTTTATGTGATCTGA-3′	67	Intron5
hHPGD Exon6			
Forward	5′-TGCAGAGTTCAGTAGATAAGAGAAGC-3′	73	Intron5
Reverse	5′-TGCTTGGAATTTAGGCAGAGA-3′	67	Intron6
hHPGD Exon7			
Forward	5′-TTGGAAGTAGCAATAGTTTAATGA-3′	68	Intron6
Reverse	5′-TCACCAAGTGCATGAAGGAA-3′	66	3′UTR

Sequencing Primer	Sequence	Binding site
hDKK1-Exon1, 2		
Forward	5′-CGTCTGCTATAACGCTCGCTGGTAG-3′	Promoter
Reverse	5′-AATTCATAGACGCTCAAAGGCTGGA-3′	Intron2
hDKK1-Exon1-S2		
Forward	5′-CCACCTTGAACTCGGTTCTC-3′	Exon1
hDKK1-Exon2-S1		
Forward	5′-AGAACGTGCTGAATGTGTGC-3′	Intron1
hDKK1-Exon3, 4		
Forward	5′-ACTTGCCCCTACCACAGTTG-3′	Intron2
Reverse	5′-GTTCCTGCCAATCACCAAGT-3′	3′UTR
hDKK1-Exon3-S1		
Forward	5′-CCTTGGATGGGTATTCCAGA-3′	Exon3
hDKK1-Exon4-S1		
Forward	5′-TCATCAGACTGTGCCTCAGG-3′	Exon4
hDKK1-Exon4-S2		
Forward	5′-AAGGTGCTGCACTGCCTATT-3′	3′UTR
hTCF-4-Exon1		
Forward	5′-TGGCTTTTCTTCCTCCTTCA-3′	5′UTR
Reverse	5′-AGAAAAAGAATCGGCGAGGT-3′	Intron1
hTCF-4-Exon9		
Forward	5′-GCTTGGGGGTTATGAGACAA-3′	Intron8
Reverse	5′-AGACATTCTGCCACCTGACC-3′	Intron9
hTCF-4-Exon10		
Forward	5′-CCTTGGCGTAATGTGTGATG-3′	Intron9
Reverse	5′-TAGCGATCCAGGAAGATGCT-3′	Intron10
hTCF-4-Exon14		
Forward	5′-ACATCCCTTAGGTGACCTCA-3′	Intron13
Reverse	5′-GGGGGCAAATTAAGAAAAGTG-3′	3′UTR

(table continues)

Table 1. *Continued*

Sequencing Primer	Sequence	Binding site
hHPGD Exon1		
Forward	5′-GCTGGCTTGACAGTTTCCTC-3′	5′UTR
Reverse	5′-CAGCCTCAGCTTCAGCAAAT-3′	Intron1
hHPGD Exon2		
Forward	5′-TTGCTGAAGCTGAGGCTGT-3′	Intron1
Reverse	5′-TCTTGCCTTTCTTTCGGTTT-3′	Intron2
hHPGD Exon3		
Forward	5′-TCCACAAACCACACATTGAGA-3′	Intron2
Reverse	5′-CCAGCTTTCTGTAACTTCCCTTT-3′	Intron3
hHPGD Exon4		
Forward	5′-TAGGCAAACCCAAAGAATCC-3′	Intron3
Reverse	5′-CACATGGGAGCAGAGACATC-3′	intron4
hHPGD Exon5		
Forward	5′-CCTGGGGAGGCAGAAAAA-3′	Intron4
Reverse	5′-TTTATTTGGTTCTTTATGTGATCTGA-3′	Intron5
hHPGD Exon6		
Forward	5′-TGCAGAGTTCAGTAGATAAGAGAAGC-3′	Intron5
Reverse	5′-TGCTTGGAATTTAGGCAGAGA-3′	Intron6
hHPGD Exon7		
Forward	5′-TTGGAAGTAGCAATAGTTTAATGA-3′	Intron6
Reverse	5′-TCACCAAGTGCATGAAGGAA-3′	3′UTR

The exons of DKK1, TCF7L2 (TCF-4), and HPGD genes were amplified via PCR in a thermal cycler using the forward and reverse primer pairs indicated in the upper list. Direct sequencing was performed with the BigDye Terminator v3.1 Cycle Sequencing Kit and sequencing primers indicated in the lower list. Binding sites of primers are also indicated.

trol reagents (Assay ID: Hs99999905) (Applied Biosystems) were used. The relative expression was calculated using the ΔΔ Ct method.[22]

For DNA microarray analysis, total RNAs were extracted from fibroblasts with the RNeasy Mini Kit (QIAGEN). For transcriptomic profiling, we used an oligonucleotide-based DNA microarray, AceGene (HumanOligoChip30K, DNA Chip Research, Yokohama, Japan). Images were analyzed with DNASIS Array (Hitachi Software Engineering, Tokyo, Japan), according to the manufacturer's instructions. Mean and SD of background levels were calculated, and genes with intensities less than mean plus 2SD of background levels were excluded from further analysis. The Cy5/Cy3 ratios of all spots on the DNA microarray were normalized by the method of global normalization.

Genetic Analysis for DKK1, TCF, *and* HPGD

Three healthy controls and two PDP patients (cases 1 and 2) were enrolled and followed up according to local

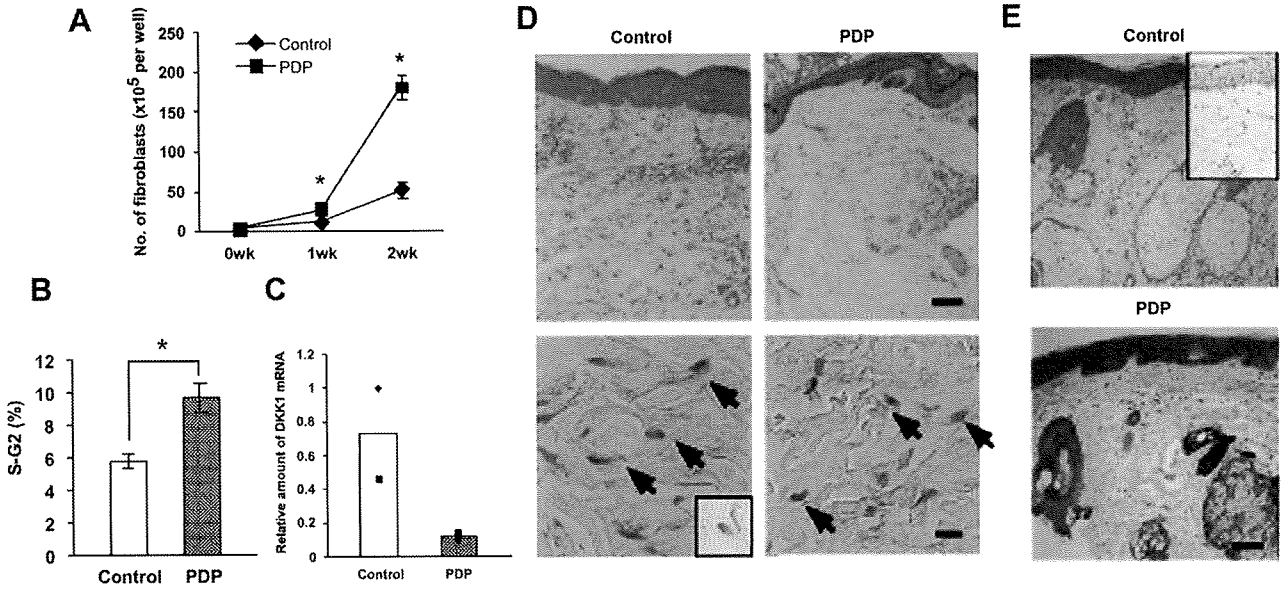

Figure 2. Characteristics of dermal fibroblasts and histology of the skin in PDP. **A:** Fibroblasts from a healthy individual (control) and an individual with PDP (case 1) (PDP) were incubated and the numbers of fibroblasts examined. **B:** The percentages of fibroblasts in S-G2 phase are shown. **C:** The levels of *DKK1* mRNA in fibroblasts from two controls and two PDPs were normalized against GAPDH, and the level of one of the control *DKK1* mRNAs is regarded as one. Filled symbols indicate two independent individuals and columns represent the average. **D** and **E:** Skin sections were stained with anti-human DKK1 (**D**) and β-catenin (**E**) antibodies. **Arrows** show the perinuclear area of fibroblasts (**D**). Scale bars: upper panels (150 μm), and lower panels, 10 μm **(D),** and 100 μm **(E).** We include that the controls incorporating non-immune serum (**D**) or mouse IgG1 (**E**) as insets show no specific reactivity. The student's *t*-test was performed (*$P < 0.05$) (**A**, **B**).

Table 2. DNA Microarray Analysis

Gene names	Accession ID	Expression levels		Difference	Fold difference
		Control	PDP		
BMP2	NM_001200_1	5.72	5.87	0.16	–
BMP3	M22491_1	ND	ND	NA	–
BMP4	NM_001202_1	7.20	7.46	0.26	–
BMP5	NM_021073_1	4.61	4.30	−0.30	–
BMP6	NM_001718_1	4.34	4.96	0.61	–
BMP7	NM_001719_1	ND	ND	NA	–
BMP8B	NM_001720_1	5.47	5.65	0.18	–
BMP10	NM_014482_1	ND	ND	NA	–
BMP15	NM_005448_1	ND	ND	NA	–
TGFB1	NM_000660_1	8.87	7.91	−0.97	–
TGFB2	NM_003238_1	4.34	5.05	0.72	–
TGFBR1	NM_004612_1	ND	ND	NA	–
TGFBR2	NM_003242_1	ND	ND	NA	–
TGFBR3	NM_003243_1	4.34	4.51	0.17	–
WNT1	NM_005430_1	6.66	5.45	−1.21	0.4
WNT2	ENSG00000105989	ND	ND	NA	–
WNT2B	NM_024494_1	6.36	6.95	0.60	–
WNT4	AY009398_1	4.33	4.35	0.03	–
WNT5A	NM_003392_1	5.36	5.85	0.50	–
WNT6	BC004329_1	5.13	4.99	−0.14	–
WNT7A	NM_004625_1	ND	ND	NA	–
WNT8B	NM_003393_1	7.27	6.88	−0.39	–
WNT9A	AB060283_1	7.36	6.92	−0.44	–
WNT9B	AF028703_1	5.69	4.47	−1.22	0.4
WNT10A	NM_025216_1	4.40	5.40	1.00	–
WNT10B	NM_003394_1	5.73	4.48	−1.25	0.4
WNT11	NM_004626_1	6.46	5.85	−0.61	–
WNT16	NM_016087_1	7.63	6.80	−0.83	–
FZD1	NM_003505_1	7.19	6.91	−0.28	–
FZD2	AB017364_1	7.05	7.01	−0.03	–
FZD3	AJ272427_1	7.51	6.85	−0.67	–
FZD3	NM_017412_1	ND	ND	NA	–
FZD4	NM_012193_1	6.09	6.49	0.41	–
FZD5	NM_003468_1	5.02	5.44	0.42	–
FZD6	NM_003506_1	5.95	6.37	0.42	–
FZD7	NM_003507_1	9.32	9.40	0.08	–
FZD8	AB043703_1	ND	ND	NA	–
DKK1	NM_012242_1	11.61	8.46	−3.15	0.1
DKK2	NM_014421_1	6.53	6.93	0.40	–
DKK3	NM_015881_1	9.24	9.15	−0.08	–
KREMEN1	AB059618_1	ND	ND	NA	–
KREMEN2	NM_024507_1	5.20	4.33	NA	–
COL1A1	K03179_1	7.57	7.90	0.34	–
COL1A2	NM_000089_1	13.54	13.98	0.44	–
COL2A1	NM_033150_1	9.46	10.09	0.63	–
COL3A1	NM_000090_1	10.26	11.43	1.17	2.3
COL4A1	NM_001845_1	8.66	7.83	−0.83	–
COL4A2	X05562_1	7.17	6.83	−0.34	–
COL4A3	U02519_1	4.54	5.04	0.49	–
COL4A4	NM_000092_1	4.73	4.30	−0.43	–
COL4A5	NM_000495_1	4.23	5.72	1.50	2.8
COL4A6	D63562_1	8.41	8.68	0.28	–
COL5A1	BC008760_1	10.35	10.25	−0.09	–
COL5A3	NM_015719_1	5.57	6.20	0.62	–
COL6A2	AY029208_1	10.90	10.62	−0.29	–
COL6A3	NM_004369_1	6.64	5.37	−1.27	0.4
COL8A1	NM_001850_1	10.47	11.09	0.61	–
COL8A2	M60832_1	5.43	5.55	0.11	–
COL9A1	NM_001851_1	6.97	6.84	−0.13	–
COL9A2	NM_001852_1	4.15	6.13	1.98	4
COL9A3	NM_001853_1	4.73	5.17	0.44	–
COL10A1	NM_000493_1	4.10	6.90	2.80	7
COL11A1	NM_001854_1	6.45	9.28	2.84	7
COL11A2	J04974_1	ND	ND	NA	–
COL12A1	NM_004370_1	4.98	6.26	1.27	2.5

(*table continues*)

Table 2. *Continued*

Gene names	Accession ID	Expression levels		Difference	Fold difference
		Control	PDP		
COL14A1	Y11711_1	4.21	5.81	1.60	3
COL15A1	NM_001855_1	ND	ND	NA	–
COL17A1	NM_000494_1	4.32	6.33	2.01	4
COL18A1	NM_030582_1	5.73	6.03	0.30	–
COL19A1	NM_001858_1	ND	ND	NA	–
FN1	X07717_1	7.10	6.69	−0.41	–
FN5	NM_020179_1	6.41	6.71	0.30	–
ELN	NM_000501_1	7.60	7.33	−0.26	–

The upper list of genes related to BMP, TGF-β, and Wnt signaling. The lower list of genes is related to collagens, fibronectins, and elastin. The mRNA expression levels of a healthy donor (control) and the individual with PDP (PDP) are normalized by LOWESS normalization, and indicated by log2. The values in Difference indicate mRNA expression levels of the individual with PDP—those of the healthy individual. The values under &lquote;Fold Difference' indicate mRNA expression levels of the individual with PDP/those of the healthy individual, ie, Log2(Difference). The symbol "–" in the Fold Difference indicates non-significant difference between the healthy donor and the individual with PDP. ND, not determined. NA, not applicable.

ethical guidelines. Genomic DNA was isolated from primary fibroblasts or peripheral blood leukocytes using proteinase K and the PCI (phenol/chloroform/isoamyl alcohol) extraction procedure. The *DKK1* (GenBank: NM012242), *TCF7L2* (*TCF-4*) (GenBank: NM030756), and *HPGD* (NM000860) genes were amplified via PCR in a thermal cycler (Eppendorf, Hamburg, Germany) using forward and reverse primer pairs (Table 1).

Amplified products were purified with the QIAquick Gel Extraction Kit (QIAGEN, Valencia, CA) or Wizard SV Gel and PCR Clean-Up System (Promega, Madison, WI) after 1.5% agarose electrophoresis. Direct sequencing was performed with the BigDye Terminator v3.1 Cycle Sequencing Kit (Applied Biosystems, Foster City, CA) and sequencing primers (Table 1) using capillary electrophoresis (ABI Prism 3130xl Genetic Analyzer; Applied Biosystems), and analyzed with ABI Prism DNA Sequencing Analysis software ver. 5.1 (Applied Biosystems) as previously described.[23]

Application of Mouse DKK1 siRNA

Mouse *DKK1* siRNA (5′-GAA CCA CAC UGA CUU CAA ATT-3′) was purchased from Nippon EGT (Toyama, Japan). siRNA duplexes were generated by mixing sense and antisense single-stranded RNA oligomers equally in an annealing buffer (NIPPON EGT).[24] Negative control siRNA (AM4611) was purchased from Ambion (Austin, TX). To impregnate mouse *DKK1* siRNA into cationized gelatin microspheres,[25] 10 μl of PBS solution (pH 7.4) containing 10 μg of mouse *DKK1* siRNA was dropped onto 1 mg of the freeze-dried cationized gelatin microspheres, kept overnight at 4°C, and added to 190 μl of PBS. Ten μl of this siRNA solution was injected intradermally into the center of the ears of 8-week-old C57BL/6j female mice (obtained from SLC, Shizuoka, Japan) using a 30-gauge needle four times every 7 days. The same amount of cationized gelatin-conjugated nonsense siRNA was applied as a negative control. The ear thickness was measured before each injection and one week after the last injection using dial-thickness gauge (PG-01, TECLOCK, Okaya, Japan). The injected area was sampled for histology and RT-PCR analysis using 6-mm punch biopsy. Mice were maintained on a 12-hour light/dark cycle under specific pathogen-free conditions. Protocols were approved by the Institutional Animal Care and Use Committee of the University of Occupational and Environmental Health.

Statistical Analysis

Data were analyzed using an unpaired two-tailed *t*-test. A *P* value of less than 0.05 was considered to be significant.

Results

Increased S-G2 Phase in Fibroblasts of PDP

Case 1 had a typical complete form of PDP (Figure 1, A and B) characterized by the triad of pachydermia, digital clubbing, and periostosis.[1–3] The histology of the skin showed thickened dermis with dense and packed collagen and elastic fibers (Figure 1, C–E), suggesting that the function of fibroblasts was enhanced in PDP. To test the proliferative activity of fibroblasts, we cultured primary fibroblasts from case 1 and a matched control, and monitored their number. As reported previously,[26] the number of PDP fibroblasts was significantly higher than that of control fibroblasts (Figure 2A). Similar results were obtained in another typical patient with PDP, case 2 (data not shown). To clarify whether it was due to enhanced cell survival or proliferation, we stained the nuclear contents of fibroblasts with 7-AAD for cell cycle analysis. The ratio of PDP fibroblasts in the cell cycle (S-G2 phase) was higher than that of control fibroblasts (Figure 2B), suggesting that the proliferation of fibroblasts was enhanced in PDP.

Decreased DKK1 Expression in PDP Fibroblasts and Skin

The above results together with the clinical phenotypes involving the skin and bone suggested the possibility that the pathogenesis of PDP is related to dysregulation of BMP, Wnt, and/or TGF-β pathways in mesenchymal cells. To efficiently compare the expression profiles of these genes between PDP fibroblasts (case 1) and matched controls,

DNA microarray analysis was performed and the complete array data were deposited in a MIAME-compliant microarray database (GSE17947). Among all genes analyzed, 2573 genes were elevated and 2346 genes were decreased more than twofold in PDP patients compared with a healthy control. The analysis revealed that the mRNA levels of *BMP* and *TGF-β* families were comparable between these two groups (Table 2). On the other hand, *WNT1*, *WNT10B*, and *DKK1* mRNAs were decreased in the patient's fibroblasts (Table 2). In particular, *DKK1* mRNA was markedly decreased. Other molecules, such as levels of *LRP5/6*, *Kremen1*, and *Kremen2* mRNA were similar between these two groups (Table 2). Moreover, the mRNA levels for collagen families, such as *COL4A5*, *COL9A2*, *COL10A1*, *COL11A1*, *COL12A1*, *COL14A1*, and *COL17A1*, were elevated, but those for *fibronectin* and *elastin* (*ELN*) families were not (Table 2). These data suggest that the PDP fibroblasts showed enhanced production of several types of collagens in addition to cell proliferation, which might explain the pathogenesis of pachydermia in PDP.

We initially confirmed the decreased *DKK1* expression using quantitative RT-PCR. Fibroblasts were primarily cultured from two PDP patients (cases 1 and 2) and two matched healthy controls. *DKK1* mRNA levels in PDP fibroblasts were consistently lower than those in the control fibroblasts (Figure 2C). We then performed immunohistochemical analysis to evaluate the expression of DKK1 protein in the PDP skin (case 1) and the control. In the normal skin, DKK1 was detected diffusely in the dermis (Figure 2D, upper panels) and notably in the cytoplasm of fibroblasts (Figure 2D, lower panels). The intensity of this expression pattern was substantially decreased in the PDP patient (case 1) (Figure 2D, lower panels). This finding was confirmed with the other PDP patient (case 2) and another matched control (data not shown). We displayed that the controls incorporating non-immune serum (inset, Figure 2D) or mouse IgG1 (inset, Figure 2E) show no specific reactivity.

The decreased expression of DKK1 in PDP suggested that Wnt signaling is enhanced in PDP. Immunohistochemical analysis revealed enhanced β-catenin expression in the PDP skin (case 1), especially around the sebaceous glands, the hair follicles, and the epidermis, and mildly in the dermis, as compared with the control (Figure 2E), supporting the augmented expression of Wnt signaling.

Suppression of Fibroblast Proliferation by DKK1

The above results indicated that Wnt signaling is enhanced in PDP through decreased DKK1 expression. However, it was still unknown whether DKK1 directly modulates the function of dermal fibroblasts. To solve this issue, we cultured dermal fibroblasts from a healthy control and the patient with PDP (case 1) in the presence or absence of human recombinant DKK1, and quantitated the DNA contents of fibroblasts by cell cycle analysis with 7-AAD. The ratio of fibroblasts in the cell cycle (S-G2 phase) was higher in the PDP patient than in the control (Figure 3, A and B). In addition, the ratio of fibroblasts with the cell cycle (S-G2 phase) was decreased by treatment with recombinant DKK1 protein in a dose-dependent manner (Figure 3B), implicating the direct involvement of DKK1 in fibroblast proliferation.

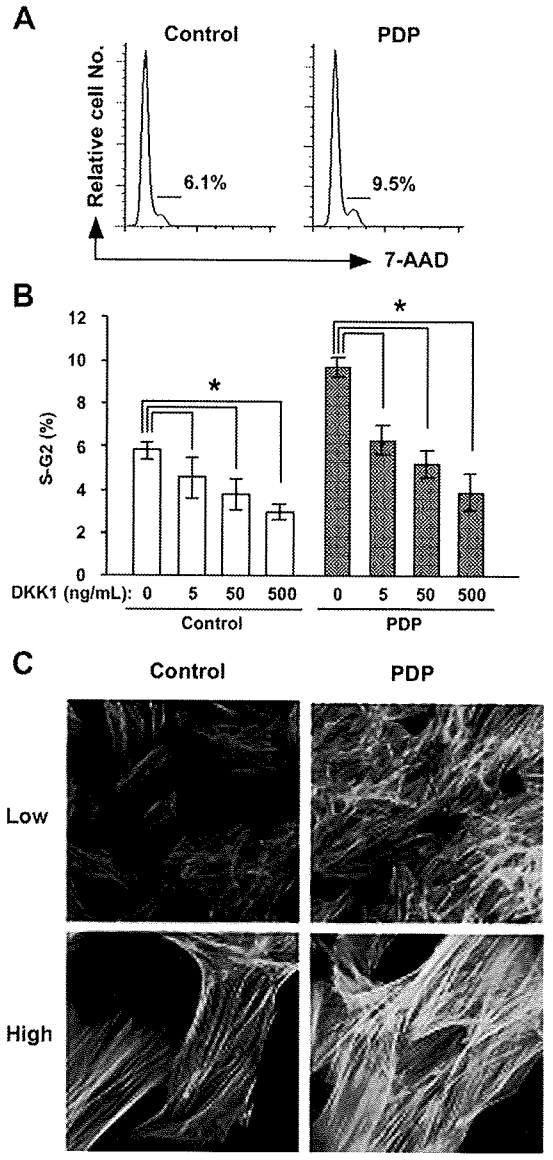

Figure 3. The effect of DKK1 on fibroblast proliferation and actin bundle formation of fibroblasts. **A, B:** The fibroblasts from a healthy individual (control) and an individual with PDP (PDP) were incubated with or without recombinant human DKK1 protein and the DNA contents of fibroblasts were evaluated with 7-AAD using flow cytometry. Representatives of FACS plots of fibroblasts from a healthy individual (control) and an individual with PDP (PDP) are shown (**A**). The percentages of fibroblasts in S-G2 phase in triplicated wells are expressed as the mean ± SD ($n = 3$). The student's *t*-test was performed between the indicated groups and $^*P < 0.05$. **C:** The actin bundle formation of cultured fibroblasts from a healthy individual (control) and an individual with PDP (PDP) were examined by staining with alexa 488-labeled phalloidin antibody 5 days after the fourth passage. Upper panels, low magnification (×10); lower panels, high magnification (×40).

Enhanced Actin Bundle Formation of Fibroblasts in PDP

Wnt signaling is also known to induce cell motility and cytoskeletal rearrangement of NIH3T3, a fibroblast cell line.[27] Therefore, we examined the actin bundle formation

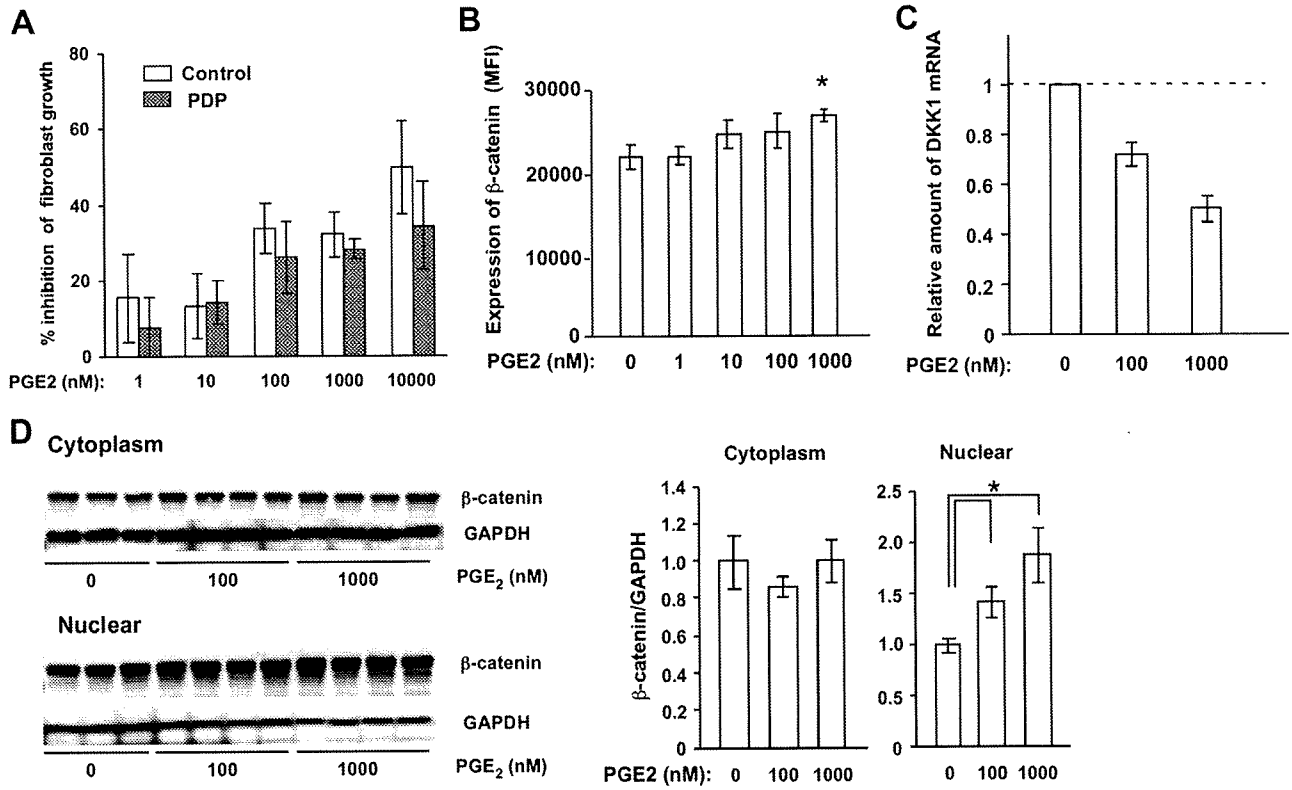

Figure 4. Effect of PGE_2 on fibroblasts. **A:** The % inhibition of the number of fibroblasts from a healthy donor and a PDP patient by the addition of PGE_2 was evaluated as (Number of fibroblasts without PGE_2 − Number of fibroblasts with PGE_2)/Number of fibroblasts without PGE_2 × 100. The growth inhibitory effect of PGE_2 is dose-dependent and comparable between these two groups. The values are expressed as the mean ± SD ($n = 3$) and are representative of two independent experiments. **B, C:** The effects of PGE_2 on β-catenin expression and *DKK1* mRNA levels in fibroblasts were evaluated. The mean fluorescent intensity (MFI) of β-catenin (**B**) and *DKK1* mRNA (**C**) in fibroblasts after exposure to PGE_2 is shown. The amount of *DKK1* mRNA relative to *GAPDH* mRNA without the addition of PGE_2 is regarded as one. The values are expressed as the mean ± SD ($n = 3$) and $^*P < 0.05$. **D:** Cytoplasm- (right panel) and nuclear- (left panel) protein samples from fibroblasts treated with or without 0, 100, and 1000 nmol/L PGE_2 for 4 days were used to determine the effect of PGE_2 on β-catenin expression. The values are expressed as the mean ± SD ($n =$ 3 to 4) and $^*P < 0.05$.

of cultured fibroblasts with phalloidin staining 5 days after the fourth passage. Fluorescent microscopy showed that the actin bundle formation of PDP fibroblasts is promoted in PDP, as the bundles were thicker and denser than those of control fibroblasts (Figure 3C).

Effect of PGE_2 on Fibroblasts

It was recently reported that the incomplete form of PDP is induced by elevated PGE_2 due to a mutation in the *HPGD* gene.[6] If this PGE_2 alteration also affects pachydermia, PGE_2 would be expected to enhance fibroblast function and proliferation. The addition of PGE_2 into the cultured medium of fibroblasts decreased the number of dermal fibroblasts from healthy donors in a dose-dependent manner as reported previously[28,29] (Figure 4A). A similar effect was observed when PGE_2 was added to the culture medium of fibroblasts from the PDP patient (case 2). To examine whether PGE_2 affects Wnt signaling in fibroblasts, we measured the amount of β-catenin in fibroblasts after exposure to PGE_2 by flow cytometry, and found that β-catenin was significantly increased in fibroblasts by the addition of PGE_2 at a dose of 1000 nmol/L (Figure 4B). In addition, the mRNA expression level of *DKK1* was significantly decreased by the addition of PGE_2 at a dose of 100 and 1000 nmol/L (Figure 4C). Moreover, to determine the effect of PGE_2 on β-catenin expression, cytoplasm- and nuclear-protein samples were prepared from fibroblasts treated with or without 0, 100, and 1000 nmol/L PGE_2 in the presence of 10 μmol/L indomethacin for 4 days. In the cytoplasm, β-catenin expression was unchanged irrespective of the addition of PGE_2. However, β-catenin expression in the nuclei was significantly increased by the treatment with 100 and 1000 nmol/L PGE_2 (Figure 4D). These results suggest that PGE_2 signaling increases nuclear β-catenin in fibroblasts.

Genetic Analysis for DKK1, TCF-4, *and* HPGD *Genes*

To address the cause of PDP, we initially analyzed the sequences of *HPGD*, and found no mutation including single nucleotide polymorphism that was different among three healthy donors and two PDP patients (data not shown). Rather, our current results suggest that the pathogenesis of the complete form of PDP may be attributable to enhanced Wnt signaling secondary to decreased DKK1 expression. Moreover, it remains uncertain how DKK1 expression is reduced in PDP. One possible mediator is TCF7L2 (TCF-4), which binds to the *DKK1* promoter, thus enhancing activity of DKK1.[30]

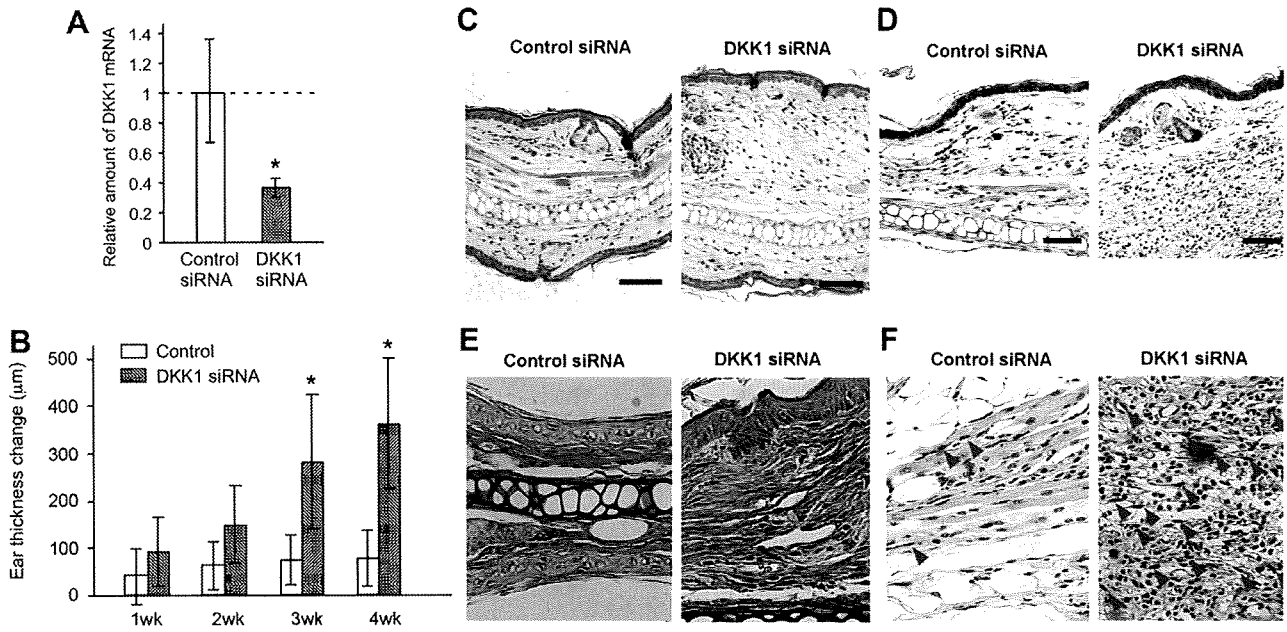

Figure 5. The effect of mouse *DKK1* siRNA on pachydermia. **A:** Mouse *DKK1* siRNA and control-scrambled siRNA (control siRNA) solutions were injected intradermally into the ears of mice four times every 7 days. The expression of *DKK1* mRNA in the skin 1 week after the last siRNA injection was evaluated by quantitative RT-PCR analysis. The mean value of *DKK1* mRNA relative to *GAPDH* mRNA treated with scrambled siRNA is regarded as one ($n = 5$). **B:** The ear thickness was measured every week before each injection and one week after the last injection. Columns show the mean ± *SD* ($n = 8$, each group) from two independent experiments. The student's *t*-test was performed between the indicated groups and $^*P < 0.05$. **C–D:** The skin from the ears one week after the last siRNA injection was fixed and stained with H&E (**C**). In addition, skin sections were stained with anti-β-catenin antibody by immunohistochemistry. Enhanced β-catenin expression is visible diffusely in the dermis of the skin treated with *DKK1* siRNA (**D**). Scale bars = 100 μm. **E:** The samples stained with Elastica van Gieson shows the thick collagen and elastic fibers in the dermis of mice treated with DKK1 siRNA. **F:** The samples are stained with proliferating cellular nuclear antigen (PCNA). **Red arrowheads** depict PCNA positive cells.

Hence, we further analyzed the sequence of *DKK1* and *TCF-4*. However, sequence analyses of the coding sequences of DKK1 and TCF-4, including exon-intron boundaries revealed no mutation (data not shown). In addition, the primers used in this study sequenced all exon-intron boundaries of *DKK1, TCF4*, and *HPGD*, but no mutation was found.

DKK1 *siRNA Enhances Ear Thickness in Mice*

Finally, we used mice to pursue direct evidence for DKK1 involvement in pachydermia. We injected a solution of mouse *DKK1* siRNA or control siRNA intradermally into the ears of mice four times every 7 days. Quantitative RT-PCR analysis revealed that this procedure successfully suppressed the expression of *DKK1* mRNA in the skin by about 60% (Figure 5A). The ear thickness was measured every week before each injection and 1 week after the last injection. The ear thickness was significantly augmented by the application of *DKK1* siRNA (Figure 5B). The histological findings showed that the dermis was thickened with increased fibroblasts (Figure 5, C–F). Consistent with these findings, enhanced β-catenin expression was observed diffusely in the dermis treated with *DKK1 si*RNA. (Figure 5D).

Discussion

We showed that Wnt/DKK1 plays a key role in the development of pachydermia in several aspects. Firstly, proliferation of fibroblasts from the PDP patients was promoted with a higher ratio in the cell cycle than compared with normal fibroblasts, and human recombinant DKK1 protein decreased their proliferation. Secondly, the expression levels of DKK1 mRNA in PDP fibroblasts and DKK1 protein in PDP skin were lower than those in healthy controls. Thirdly, β-catenin intensity in the skin from PDP was pronounced by immunohistochemistry. Finally, application of mouse *DKK1* siRNA increased the thickness of the skin in accordance with the elevated β-catenin levels. These results suggest that enhanced Wnt signaling is related to the development of pachydermia.

Pachydermia is one of the clinical manifestations of the complete form of PDP, which involves both skin and bone. For example, BMP, TGF-β, and Wnt families are the possible molecules responsible for the changes in both organs. There are several congenital diseases related to both organs, such as basal cell nevus syndrome, synovitis acne pustulosis hyperostosis ostitis syndrome, Klippel-Trenaunay-Weber syndrome, and Buschke-Ollendorff syndrome.[31–33] Bushchke-Ollendorff syndrome, in which osteopoikilosis is associated with connective tissue nevi, is particularly of note, since mutations in *LEMD3*, a gene implicated in BMP signaling, are candidates for its pathogenesis.[34] However, we could not detect a significant difference in mRNA expression for *BMP* or *TGF-β* families between PDP and control fibroblasts by DNA microarray analysis.

Recently, the incomplete form of PDP was attributed to elevated PGE_2 due to the mutation of *HPGD*. The skeletal phenotype of PDP, particularly clubbing and periostosis, can clearly be explained by elevated PGE_2, since it is well known that PGE_2 stimulates the activity of both os-

teoclasts and osteoblasts,[35] leading to bone deposition (periostosis) and resorption (acro-osteolysis), respectively. However, we could not detect a mutation in HPGD. In addition, the level of serum PGE_2 from one of our PDP cases (case 1) was within the normal range (data not shown). In fact, long-term therapeutic administration of exogenous PGE_2 for skin ulcers secondary to systemic sclerosis, arteriosclerosis obliterans, and Buerger diseases does not induce pachydermia, sebaceous hyperplasia, or velvet coloration of the skin as adverse effects. Moreover, the addition of PGE_2 into the fibroblast culture did not induce proliferation. Therefore, it remains unknown how the skin manifestations of PDP are induced.

Here we focused on Wnt signaling in the development of pachydermia. Fibroblasts from PDP skin and bone marrow-derived fibroblasts of PDP patients are known to grow faster than those of healthy donors.[26,36] The transfection of *DKK1* into cultured mouse fibroblasts, NIH3T3, blocked WNT2-induced cell growth and the WNT2-induced increase in uncomplexed β-catenin.[37] WNT3a induced motility and cytoskeletal rearrangement of NIH3T3 cells.[27] These previous reports suggest that enhanced Wnt/β-catenin signaling promotes fibroblast proliferation and cytoskeletal rearrangement. In fact, we found that the frequency of PDP fibroblasts in cycle was increased, and that actin bundle formation was more pronounced in PDP fibroblasts. Moreover, the addition of human recombinant *DKK1* consistently suppressed the fibroblast proliferation.

The source of DKK1 and how it works in the skin are issues that remain to be clarified. According to our immunohistochemical analysis, the major source of DKK1 in the skin seems to be fibroblasts, because the DKK1 expression in fibroblasts was low in PDP. Since DKK1 is a secreted antagonist and may affect bystander cells in the vicinity of fibroblasts, the dysregulated production of DKK1 possibly modulates the functions of not only fibroblasts but also other cells, such as keratinocytes and melanocytes. It was reported that high *DKK1* expression by dermal fibroblasts in the palms and soles inhibits the function of melanocytes via suppression of β-catenin and microphthalmia-associated transcription factor, and enhances keratinocyte proliferation.[16,17,38] Mice with an overexpression of *DKK1* in skin consistently lacked formation of appendages, such as hair follicles, and the mice had no skin pigmentation on the trunk.[18]

The role of DKK1 has been more extensively studied in bone than in the skin. DKK1 is known to inhibit osteoblast differentiation, and the overproduction of DKK1 was noted in osteolytic bone lesions of patients with multiple myeloma.[39] The elevated *DKK1* levels in bone marrow plasma and peripheral blood from the patients were correlated with the presence of focal bone lesions. Recombinant human *DKK1* inhibited the differentiation of osteoblast precursor cells *in vitro*.[40,41] These previous observations could explain the periostosis in PDP possibly secondary to decreased *DKK1* expression. Since fibroblasts and osteoblasts are derived from mesenchymal origin, they seem to share in common the mechanism of differentiation and proliferation. Although we did not address the relationship between DKK1 and the skeletal phenotype in PDP, it would be of interest to analyze the function of osteoblasts in PDP.

The next question is how Wnt signaling is enhanced. One possibility provided by our present study is the suppression of DKK1 expression in fibroblasts. The mechanism by which DKK1 is down-regulated in PDP remains to be elucidated. It can be hypothesized that there is a mutation in *DKK1* or molecules controlling *DKK1* expression, such as TCF-4. However, no mutation was detected in either exons of DKK1 or TCF-4 genes. Therefore, in the present study, we could not determine the genetic mechanism responsible for the complete form of PDP and/or pachydermia. Given the defect in PDP appears to altered expression of DKK1, it will be of interest in future studies to analyze the regulatory regions of DKK1, especially around the TCF binding sites, an issue which remains to be clarified.

On the other hand, the Wnt/β-catenin pathway is known to increase *DKK1* mRNA and protein, thus initiating a negative feedback loop.[42] It can be hypothesized that this negative feedback regulation might be dysregulated in PDP. Moreover, due to this negative feedback system, DKK1 can work as a tumor suppressor gene in some types of neoplasia.[42,43] Hypertrophic osteoarthritis is occasionally induced by a variety of thoracoabdominal, sometimes malignant, conditions. The relationship between decreased DKK1 expression and secondary hypertrophic osteoarthritis in association with malignancy may be an interesting issue to pursue.

It still remains unclear whether PDP in our cases could be attributed to the mutation in HPGD or not. Of note is that our cases were diagnosed as the complete form of PDP including pachydermia and adolescent onset, but that the cases with HPGD mutation had the incomplete form of PDP without pachydermia and with early onset (within the first year of their lives). The onset of the PDP is bimodal. The first peak is during the first year of the life and the second at the age of 15 years.[3,44] Therefore, the pathogenesis of PDP might be subdivided into at least two groups. However, further clinical studies in combination with HPGD mutation analysis will be required to clarify this.

In PDP, clinical cutaneous manifestations include pachydermia, seborrhea, and velvet colored skin. At present, we could not show direct evidence that all of the phenotypes of PDP were induced by enhanced Wnt signaling secondary to the suppressed expression of DKK1. In addition, the number of cases in our study was limited. However, our findings, together with those of previous studies suggest that the Wnt signaling pathway was promoted in accordance with decreased DKK1 expression, leading to increased fibroblast proliferation, enhanced pigmentation of the skin, and adnexal hyperplasia.

Acknowledgments

We thank Ms. Rie Murase and Dr. Yosuke Okada for technical assistance, and Dr. Tatsuya Ishibe for discussion.

References

1. Vogl A, Goldfischer S: Pachydermoperiostosis: primary or idiopathic hypertrophic osteoarthropathy. Am J Med 1962, 33:166–187
2. Shawarby K, Ibrahim MS: Pachydermoperiostosis. A review of literature and report on four cases. Br Med J 1962, 1:763–766
3. Rimoin DL: Pachydermoperiostosis (idiopathic clubbing and periostosis): genetic and physiologic considerations. N Engl J Med 1965, 272:923–931
4. Jajic I, Jajic Z, Grazio S: Minor but important symptoms and signs in primary hypertrophic osteoarthropathy. Clin Exp Rheumatol 2001, 19:357–358
5. Touraine A, Solente G, Gole A: Un syndrome osteodermopathique: la pachydermie plicaturee avec pachyperiostose des extremites. Presse Med 1935, 43:1820–1824
6. Uppal S, Diggle CP, Carr IM, Fishwick CW, Ahmed M, Ibrahim GH, Helliwell PS, Latos-Bielenska A, Phillips SE, Markham AF, Bennett CP, Bonthron DT: Mutations in 15-hydroxyprostaglandin dehydrogenase cause primary hypertrophic osteoarthropathy. Nat Genet 2008, 40: 789–793
7. Castori M, Sinibaldi L, Mingarelli R, Lachman RS, Rimoin DL, Dallapiccola B: Pachydermoperiostosis: an update. Clin Genet 2005, 68:477–486
8. Kornak U, Mundlos S: Genetic disorders of the skeleton: a developmental approach. Am J Hum Genet 2003, 73:447–474
9. Botchkarev VA, Sharov AA: BMP signaling in the control of skin development and hair follicle growth. Differentiation 2004, 72:512–526
10. Zorn AM: Wnt signalling: antagonistic Dickkopfs. Curr Biol 2001, 11:R592–595
11. Kawano Y, Kypta R: Secreted antagonists of the Wnt signalling pathway. J Cell Sci 2003, 116:2627–2634
12. Mao B, Wu W, Davidson G, Marhold J, Li M, Mechler BM, Delius H, Hoppe D, Stannek P, Walter C, Glinka A, Niehrs C: Kremen proteins are Dickkopf receptors that regulate Wnt/beta-catenin signalling. Nature 2002, 417:664–667
13. Mao B, Wu W, Li Y, Hoppe D, Stannek P, Glinka A, Niehrs C: LDL-receptor-related protein 6 is a receptor for Dickkopf proteins. Nature 2001, 411:321–325
14. Glinka A, Wu W, Delius H, Monaghan AP, Blumenstock C, Niehrs C: Dickkopf-1 is a member of a new family of secreted proteins and functions in head induction. Nature 1998, 391:357–362
15. Grotewold L, Ruther U: The Wnt antagonist Dickkopf-1 is regulated by Bmp signaling and c-Jun and modulates programmed cell death. EMBO J 2002, 21:966–975
16. Yamaguchi Y, Itami S, Watabe H, Yasumoto K, Abdel-Malek ZA, Kubo T, Rouzaud F, Tanemura A, Yoshikawa K, Hearing VJ: Mesenchymal-epithelial interactions in the skin: increased expression of dickkopf1 by palmoplantar fibroblasts inhibits melanocyte growth and differentiation. J Cell Biol 2004, 165:275–285
17. Yamaguchi Y, Passeron T, Watabe H, Yasumoto K, Rouzaud F, Hoashi T, Hearing VJ: The effects of dickkopf 1 on gene expression and Wnt signaling by melanocytes: mechanisms underlying its suppression of melanocyte function and proliferation. J Invest Dermatol 2007, 127:1217–1225
18. Andl T, Reddy ST, Gaddapara T, Millar SE: WNT signals are required for the initiation of hair follicle development. Dev Cell 2002, 2:643–653
19. Masuda K, Moriwaki S, Takigawa M, Furukawa F, Higashishiba T, Fukamizu H: A case of pachydermoperiostosis. Rinsho Hifuka (Japanese) 2000, 54:398–401
20. Kabashima K, Banks TA, Ansel KM, Lu TT, Ware CF, Cyster JG: Intrinsic lymphotoxin-beta receptor requirement for homeostasis of lymphoid tissue dendritic cells. Immunity 2005, 22:439–450
21. Kabashima K, Haynes NM, Xu Y, Nutt SL, Allende ML, Proia RL, Cyster JG: Plasma cell S1P1 expression determines secondary lymphoid organ retention versus bone marrow tropism. J Exp Med 2006, 203:2683–2690
22. Livak KJ, Schmittgen TD: Analysis of relative gene expression data using real-time quantitative PCR and the 2[-Delta Delta C(T)] method. Methods 2001, 25:402–408
23. Kabashima K, Sakabe J, Yamada Y, Tokura Y: "Nagashima-type" keratosis as a novel entity in the palmoplantar keratoderma category. Arch Dermatol 2008, 144:375–379
24. Maekawa M, Yamamoto T, Tanoue T, Yuasa Y, Chisaka O, Nishida E: Requirement of the MAP kinase signaling pathways for mouse preimplantation development. Development 2005, 132:1773–1783
25. Kushibiki T, Matsumoto K, Nakamura T, Tabata Y: Suppression of tumor metastasis by NK4 plasmid DNA released from cationized gelatin. Gene Ther 2004, 11:1205–1214
26. Matucci-Cerinic M, Sacerdoti L, Perrone C, Carossino A, Cagnoni ML, Jajic I, Lotti T: Pachydermoperiostosis (primary hypertrophic osteoarthropathy): in vitro evidence for abnormal fibroblast proliferation. Clin Exp Rheumatol 1992, 10 Suppl 7:57–60
27. Kim SE, Choi KY: EGF receptor is involved in WNT3a-mediated proliferation and motility of NIH3T3 cells via ERK pathway activation. Cell Signal 2007, 19:1554–1564
28. Fine A, Goldstein RH: The effect of PGE2 on the activation of quiescent lung fibroblasts. Prostaglandins 1987, 33:903–913
29. Korn JH, Halushka PV, LeRoy EC: Mononuclear cell modulation of connective tissue function: suppression of fibroblast growth by stimulation of endogenous prostaglandin production. J Clin Invest 1980, 65:543–554
30. Niida A, Hiroko T, Kasai M, Furukawa Y, Nakamura Y, Suzuki Y, Sugano S, Akiyama T: DKK1, a negative regulator of Wnt signaling, is a target of the beta-catenin/TCF pathway. Oncogene 2004, 23:8520–8526
31. Kahn MF, Chamot AM: SAPHO syndrome. Rheum Dis Clin North Am 1992, 18:225–246
32. Oduber CE, van der Horst CM, Hennekam RC: Klippel-Trenaunay syndrome: diagnostic criteria and hypothesis on etiology. Ann Plast Surg 2008, 60:217–223
33. Ehrig T, Cockerell CJ: Buschke-Ollendorff syndrome: report of a case and interpretation of the clinical phenotype as a type 2 segmental manifestation of an autosomal dominant skin disease. J Am Acad Dermatol 2003, 49:1163–1166
34. Hellemans J, Preobrazhenska O, Willaert A, Debeer P, Verdonk PC, Costa T, Janssens K, Menten B, Van Roy N, Vermeulen SJ, Savarirayan R, Van Hul W, Vanhoenacker F, Huylebroeck D, De Paepe A, Naeyaert JM, Vandesompele J, Speleman F, Verschueren K, Coucke PJ, Mortier GR: Loss-of-function mutations in LEMD3 result in osteopoikilosis. Buschke-Ollendorff syndrome and melorheostosis. Nat Genet 2004, 36:1213–1218
35. Raisz LG, Pilbeam CC, Fall PM: Prostaglandins: mechanisms of action and regulation of production in bone. Osteoporos Int 1993, 3 Suppl 1:136–140
36. Fontenay-Roupie M, Dupuy E, Berrou E, Tobelem G, Bryckaert M: Increased proliferation of bone marrow-derived fibroblasts in primitive hypertrophic osteoarthropathy with severe myelofibrosis. Blood 1995, 85:3229–3238
37. Fedi P, Bafico A, Nieto Soria A, Burgess WH, Miki T, Bottaro DP, Kraus MH, Aaronson SA: Isolation and biochemical characterization of the human Dkk-1 homologue, a novel inhibitor of mammalian Wnt signaling. J Biol Chem 1999, 274:19465–19472
38. Yamaguchi Y, Passeron T, Hoashi T, Watabe H, Rouzaud F, Yasumoto K, Hara T, Tohyama C, Katayama I, Miki T, Hearing VJ: Dickkopf 1 (DKK1) regulates skin pigmentation and thickness by affecting Wnt/beta-catenin signaling in keratinocytes. FASEB J 2008, 22:1009–1020
39. Qiang YW, Endo Y, Rubin JS, Rudikoff S: Wnt signaling in B-cell neoplasia. Oncogene 2003, 22:1536–1545
40. Tian E, Zhan F, Walker R, Rasmussen E, Ma Y, Barlogie B, Shaughnessy JD Jr: The role of the Wnt-signaling antagonist DKK1 in the development of osteolytic lesions in multiple myeloma. N Engl J Med 2003, 349:2483–2494
41. Morvan F, Boulukos K, Clement-Lacroix P, Roman Roman S, Suc-Royer I, Vayssiere B, Ammann P, Martin P, Pinho S, Prognonec P, Mollat P, Niehrs C, Baron R, Rawadi G: Deletion of a single allele of the Dkk1 gene leads to an increase in bone formation and bone mass. J Bone Miner Res 2006, 21:934–945
42. Gonzalez-Sancho JM, Aguilera O, Garcia JM, Pendas-Franco N, Pena C, Cal S, Garcia de Herreros A, Bonilla F, Munoz A: The Wnt antagonist DICKKOPF-1 gene is a downstream target of beta-catenin/TCF and is downregulated in human colon cancer. Oncogene 2005, 24:1098–1103
43. Polakis P: Wnt signaling and cancer. Genes Dev 2000, 14:1837–1851
44. Matucci-Cerinic M, Lotti T, Jajic I, Pignone A, Bussani C, Cagnoni M: The clinical spectrum of pachydermoperiostosis (primary hypertrophic osteoarthropathy). Medicine (Baltimore) 1991, 70:208–214

TISSUE ENGINEERING: Part A
Volume 00, Number 00, 2010
© Mary Ann Liebert, Inc.
DOI: 10.1089/ten.tea.2009.0322

Original Article

Controlled Release of Bone Morphogenetic Protein-2 Enhances Recruitment of Osteogenic Progenitor Cells for *De Novo* Generation of Bone Tissue

Yu Kimura, Ph.D.,[1] Nobuhiko Miyazaki, M.Eng.,[1] Naoki Hayashi, M.Eng.,[1]
Satoru Otsuru, M.D., Ph.D.,[2] Katsuto Tamai, M.D., Ph.D.,[2] Yasufumi Kaneda, M.D., Ph.D.,[2]
and Yasuhiko Tabata, Ph.D., D.Med.Sci., D.Pharm.[1]

The objective of this study was to evaluate the cellular contribution to the phenomenon of *de novo* generation of bone tissue induced by the controlled release of bone morphogenetic protein-2 (BMP-2). Gelatin hydrogels (2 mg) incorporating BMP-2 (3 μg) with different water contents were subcutaneously implanted into the back of enhanced green fluorescent protein-chimeric mice to induce the ectopic *de novo* generation of bone tissue. The hydrogels incorporating BMP-2 could release BMP-2 at different time profiles. When evaluated radiologically and histologically, the ectopic *de novo* generation of bone tissue was induced by the controlled release of BMP-2 from the hydrogels around the hydrogel-implanted site. The relative percentage number of green fluorescent protein- to osteocalcin-positive cells recruited into the *de novo* generated bone tissue depended on the BMP-2 release profile. The higher the percentage, the stronger was the *de novo* generation of bone tissue. These findings indicate that bone marrow-derived osteoblast progenitor cells were recruited from the blood circulation by BMP-2 release and consequently contributed to the ectopic *de novo* generation of bone tissue. It is conceivable that the local concentration of BMP-2 modifies the recruitment profile of progenitor cells with an osteogenic potential around the release site of BMP-2, resulting in regulated volume of *de novo* generated bone tissue.

Introduction

TISSUE ENGINEERING has been vigorously investigated over the last 20 years to experimentally demonstrate the biomedical feasibility of regeneration in medical therapy. The key components are cells, the scaffolds for cells attachment, proliferation, or differentiation, and biosignaling molecules for cell proliferation and differentiation. Various precursor or stem cells have been extensively studied and the mechanisms of their differentiation into specific cell lineages have been clarified recently.[1,2] Among the well-recognized mechanisms, it has been demonstrated that several soluble factors interact with their cellular receptor and subsequently start the intracellular signals required for specific gene expression. In addition, the matrix present around cells, so-called extracellular matrix, also plays an important role in the activation of signals and their biological functions.[3–5]

Recently, some research reports strongly suggest that stem or precursor cells circulating in the blood and body are originally present for hematopoiesis, vascularization, or mesenchymal tissue regeneration.[6–15] Therefore, it is highly conceivable that a promoted recruitment of cells that are inherently present in the body to a body site results in cell-based tissue regeneration at the site. If the *in vivo* recruitment or fate of cells can be regulated by making use of their recruitment mechanism, tissue regeneration based on the cells present in the body can be achieved. We have developed gelatin hydrogels for the controlled release of various biosignaling molecules, such as growth factors, chemokines, and genes, and succeeded in the regeneration and repairing of various tissues.[16] Among them, it is well-known that bone morphogenetic protein-2 (BMP-2) is a strong inducer of bone tissue formation through mesenchymal cell infiltration, differentiation of mesenchymal cells into chondrocytes, diminishment of chondroid tissue, and generation of bone tissue.[17–19] Many researches have been reported for the complete regeneration of bone tissue with BMP-2.[20] In addition, it has been reported that BMP-2 is able to enhance the cells' mobilization.[21] This activity is promising and useful from the viewpoint that tissue regeneration can be achieved through the recruitment of cells originally present in the body.

[1]Department of Biomaterials, Institute for Frontier Medical Sciences, Kyoto University, Kyoto, Japan.
[2]Department of Molecular therapeutics, Graduate School of Medicine, Osaka University, Osaka, Japan.

The objective of this study was to evaluate BMP-2-induced *de novo* generation of bone tissue in terms of cell recruitment. Previous research reports have demonstrated the contribution of bone marrow for bone fracture healing through hematoma formation.[22–25] Although they indicated the possible contribution of growth factors in hematoma or bone marrow cells to fracture healing, the characterization of cells contributing for *de novo* generation of bone tissue was not clarified. In this study, BMP-2 was incorporated into gelatin hydrogels with different degradabilities for the controlled release in different profiles. After the hydrogels incorporating BMP-2 were implanted subcutaneously, ectopic *de novo* generation of bone tissue was evaluated by radiological and histological examinations. We examined the effect of BMP-2 release profile on the recruitment of bone marrow-derived osteoblast progenitor cells at the release site of BMP-2 and the consequent *de novo* generation of bone tissue.

Materials and Methods

Materials

A gelatin sample with an isoelectric point of 9.0 was isolated from the porcine skin by an acidic process of collagen (Nitta Gelatin, Osaka, Japan). $Na^{125}I$ (NEZ-033H, >12.95 GBq/mL) was purchased from Perkin-Elmer Life Sciences (Boston, MA). Other chemicals were obtained from Wako Pure Chemical Industries (Osaka, Japan) and used without further purification.

Preparation of gelatin hydrogels

Chemically crosslinked gelatin hydrogels with glutaraldehyde (GA) were prepared according to a previously reported method.[26] Briefly, aqueous solution of 3 wt% gelatin (pH 5.0) was mixed with GA at a final concentration of 0.16 and 0.09 wt%, respectively, followed by incubation at 4°C for 12 h for gelatin crosslinking. The gelatin hydrogel crosslinked was treated with 0.1 M glycine solution to block the residual aldehyde groups. After washing with double-distilled water for three times, the hydrogels were freeze-dried. The crosslinking extent of prepared hydrogels was evaluated by measuring the water content according to a previously described method.[27] The water contents of hydrogels prepared with higher and lower GA concentrations were 97.5 ± 0.1 and 99.3 ± 0.0 wt%, respectively.

In vivo *release test of BMP-2 from gelatin hydrogels*

All the animal experiments were performed according to the Institutional Guidance of Kyoto University on Animal Experimentation and with permission from the Animal Experiment Committee of the Institute for Frontier Medical Science, Kyoto University. All the surgical procedures were performed under continuous inhalation anesthesia using isoflurane (Forane®; Abbott Japan, Osaka, Japan) with 400 Anesthesia Unit (Univentor, Zejtun, Malta).

Human recombinant BMP-2 (Yamanouchi Pharmaceutical, Tokyo, Japan) was radioiodinated through the conventional chloramine T method as previously described.[28] Briefly, 5 μL of $Na^{125}I$ was added to 200 μL of BMP-2 solution (150 μg/mL) in 0.5 M potassium phosphate buffer (pH 7.5) containing 0.5 M sodium chloride. Then, 0.2 mg/mL of chloramine-T in the same buffer (100 μL) was added to the solution mixture. After agitation at room temperature for 2 min, 100 μL of phosphate-buffered saline (PBS; pH 7.4) containing 0.4 mg of sodium metabisulfate was added to the reaction solution to stop radioiodination. The reaction mixture was passed through a PD-10 desalting column (GE Healthcare Life Sciences, Giles, UK) to remove the uncoupled, free ^{125}I molecules from the ^{125}I-labeled BMP-2 (9.0 μg/mL; removal ratio of free ^{125}I = 97.0%).

PBS containing ^{125}I-labeled BMP-2 (27.4 μL, 9.0 μg/mL) and PBS containing nonlabeled BMP-2 (2.6 μL, 1 mg/mL) were mixed and dropped onto 2 mg of freeze-dried gelatin hydrogels, followed by incubation at 4°C for 12 h, to allow to swell into the hydrogel. Following the implantation of gelatin hydrogels incorporating ^{125}I-labeled BMP-2 into the back subcutis of 6-week-old, female ddY mice (18–20 g body weight; Shimizu Laboratory Supply, Kyoto, Japan), tissue around the implanted site was extracted at different time intervals after hydrogel implantation, and the tissue radioactivity was counted by a gamma counter to estimate the *in vivo* time profiles of BMP-2 release ($n = 3$, at each time point).

Preparation of green fluorescent protein-chimeric mice

C57BL/6 transgenic mice that ubiquitously express enhanced green fluorescent protein (GFP) under the Cyto-Megalovirus (CMV) early enhancer/chicken β actin (CAG) promoter were provided by RIKEN BRC through the National Bio-Resource Project of the MEXT, Japan. Preparation of chimeric mice was performed according to a previously reported procedure.[29] Briefly, bone marrow cells were isolated from 8- to 10-week-old, male transgenic mice under sterile conditions.[30] The cells were incubated with CD90.2 microbeads (no. 130-049-101; Miltenyi Biotec, Auburn, CA) and RPMI 1640 medium at 8°C for 20 min and passed through large depletion (LD) column with Midi MACS system (no. 130-042-901; Miltenyi Biotec) for depletion of CD-90.2-positive T cells and prevention of subsequent autoimmune attack. Eight- to 10-week-old, female C57BL/6 mice were irradiated lethally with 10 Gy of gamma ray. For total bone marrow transplantation, 5×10^6 of bone marrow cells prepared from GFP transgenic mice was intravenously administered to recipient irradiated mice. After the transplantation, the mice were bred for 10 weeks to complete the replacement of bone marrow cells to GFP-positive cells. The replacement ratio of bone marrow cells was 93.2% ± 1.5% when evaluated by the fluorescence-associated cell sorter method (FACS Calibur; BD Bioscience, Franklin Lakes, NJ).

In vivo *assay of* de novo *generation of bone tissue*

BMP-2 was dissolved in PBS at 100 μg/mL and the solution (30 μL) was dropped on the gelatin hydrogel (2 mg) to allow it to swell into the hydrogel. After incubation of the hydrogels incorporating BMP-2 at 4°C for 12 h, the hydrogels were implanted to the back subcutis of GFP-chimeric mice. As a control, gelatin hydrogels incorporating PBS were similarly implanted to the back of the mice. Then, the tissue around the implanted sites was extracted at different time intervals after hydrogel implantation, and the fluorescent images of tissues were obtained by a digital microscope (Multiviewer System VB-S20; Keyence, Osaka, Japan). *De novo* generation of bone tissue was radiologically exam-

ined by a soft X-ray machine (Hitex-100; Hitachi, Tokyo, Japan) at 54 kV and 2.5 mA for 20 s. Then the extracted tissues were fixed with 4% paraformaldehyde at 4°C for 48 h, and the bone tissue was decalcified with PBS containing 9 wt% ethylenediamine tetraacetic acid disodium salt and 10 wt% ethylenediamine tetraacetic acid tetrasodium salt (EDTA solution) at 4°C for 6 days. The EDTA solution was changed every other day. After decalcification, the pellets were equilibrated in PBS containing 15 wt% sucrose for 12 h and then in PBS containing 30 wt% sucrose for 12 h, embedded in Tissue-Tek OCT Compound (Sakura Finetek, Tokyo, Japan), frozen on dry ice, and stored at −80°C. For the histological examinations, 6-μm-thick sections were cut with a cryostat (Leica Microsystems AG, Wetzlar, Germany) at the portion of implanted site as central as possible, followed by staining with hematoxylin and eosin. The area of newly formed bone tissue was assessed in terms of histological image analysis using the computer program Image-Pro Plus 3.01 (Media-Cybernetics, Silver Spring, MD).

Immunofluorescence staining

After washing with PBS, the sections (6 μm thickness) were blocked with a normal goat serum for 1 h at room temperature before incubation with a rabbit polyclonal anti-mouse osteocalcin antibody (1:250; Takara Bio, Shiga, Japan) for 1 h at room temperature. Then the sections were stained with a tetramethylrhodamine-isothiocyanate-conjugated goat anti-rabbit IgG (Molecular Probes, Eugene, OR) for 1 h at room temperature. After washing with PBS, the sections were mounted with Vectashield® (Vector Laboratories, Burlingame, CA). Fluorescent images were obtained using an epifluorescent microscope (AX-80; Olympus, Tokyo, Japan), and the relative percentage number of GFP-positive cells to osteocalcin-positive cells in each image was calculated manually by observing the images. Three areas of interest ($100 \times 100\ \mu m^2$) were chosen randomly from each fluorescent image (at least four images per each experimental group) and the number of GFP- and osteocalcin-positive cells were counted.

In vitro *migration assay*

Bone marrow cells (3×10^6 cells/cm^2) isolated from the transgenic mice described earlier were plated onto cell culture dish (no. 430167; Corning Incorporated, Corning, NY) with alpha minimum essential medium (αMEM; Sigma-Aldrich, St. Louis, MO) containing 15 vol% fetal bovine serum (FBS) and cultured at 37°C and 5% CO_2–95% air atmospheric pressure. The cells were flushed with PBS at 3 days after seeding to remove unattached blood cells and cultured till subconfluent condition for further experiment. The medium was changed to αMEM without serum at 24 h before the migration assay experiment. The cells were trypsinized and plated onto the HTS® fluoroblok inserts (1.3×10^3 cells/mm^2; Falcon no. 351552 with 8-μm-diameter pore; Becton Dickinson, Franklin Lakes, NJ) with αMEM containing 0.5 vol% FBS. The bottom side of the inserts contacted αMEM containing 15 or 0.5 vol% FBS, 100 ng/mL of recombinant human stromal cell-derived factor-1 (SDF-1; no. 350-NS/CF; R&D systems, Minneapolis, MN), BMP-2, or recombinant human placental growth factor (PlGF; no. 264-PG; R&D systems) with 0.1 vol% bovine serum albumin. After 24 h culture, cells that migrated to the bottom side were counted from fluorescent photographs taken by an epifluorescent microscope (IX-70; Olympus). The number of cells in six images (0.594 mm^2 per each image) were counted.

Statistical analysis

All the results were statistically analyzed by the unpaired Student's t-test and $p < 0.05$ was considered to be statistically significant. Data were expressed as the mean ± standard deviation.

Results

De novo *generation of bone tissue by gelatin hydrogels incorporating BMP-2*

Figure 1 shows the time profiles of *in vivo* radioactivity remaining after implantation of gelatin hydrogels incorporating ^{125}I-labeled BMP-2 with different water contents. The gelatin hydrogels with higher water content released BMP-2 faster than those with lower water content.

Figure 2 shows the soft X-ray radiophotographs of implanted sites at 2 weeks after the implantation of gelatin hydrogels incorporating 3 μg of BMP-2 or PBS. A radio-opacity portion was observed at the center of tissues implanted with gelatin hydrogels incorporating BMP-2, although the influence of water content on the extent was not observed. On the contrary, no radio-opacity was observed for the BMP-2-free gelatin hydrogels.

Figure 3a–c shows the histological images of the implanted site at 2 weeks after implantation of the gelatin hydrogels incorporating 3 μg of BMP-2 or PBS. Figure 3d shows the histological image of the implanted site at 7 weeks after implantation of the gelatin hydrogel incorporating BMP-2.

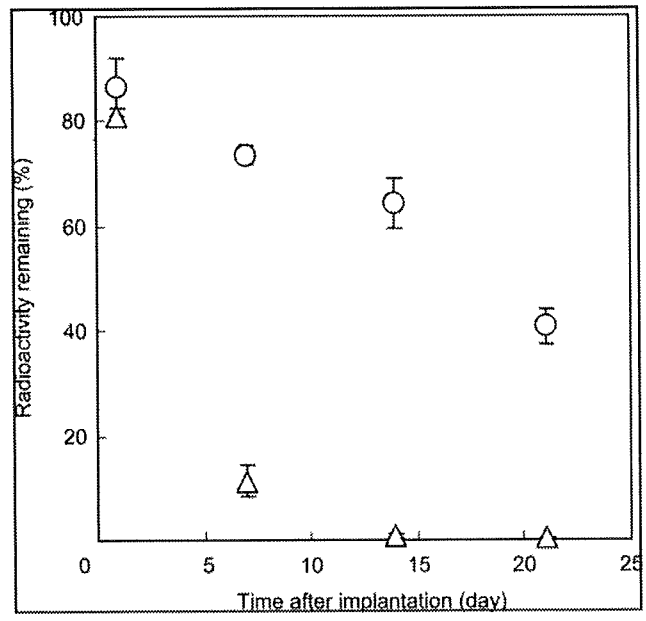

FIG. 1. *In vivo* release profiles of BMP-2 from gelatin hydrogels with water content of 97.5 wt% (○) and 99.3 wt% (△). BMP, bone morphogenetic protein.

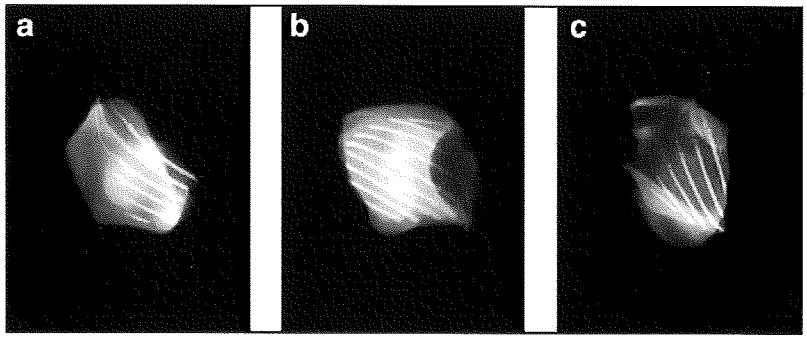

FIG. 2. Soft X-ray radiophotographs of tissues around the implanted site at 2 weeks after implantation of (**a**) the gelatin hydrogel incorporating BMP-2 (3 μg) with a water content of 97.5 wt%, (**b**) the gelatin hydrogel incorporating BMP-2 (3 μg) with a water content of 99.3 wt%, and (**c**) the gelatin hydrogel incorporating PBS with a water content of 97.3 wt%. PBS, phosphate-buffered saline.

After implantation, mature bone tissues with a bone marrow-like structure containing many inflammatory cells, blood cells, and adipocytes (Fig. 3e) were observed. The implanted gelatin hydrogel was completely degraded and was not detected in the section. Figure 4 shows the area of newly formed bone tissue at the implanted site of gelatin hydrogels incorporating BMP-2. After the implantation of gelatin hydrogel incorporating BMP-2 with a water content of 99.3 wt%, the *de novo* generation of bone tissue was observed only at 2 weeks, but thereafter the tissue disappeared. On the contrary, the implantation of hydrogels incorporating BMP-2 with a water content of 97.5 wt% induced significant *de novo* generation of bone tissue and the bone tissue was retained even at 7 weeks after implantation.

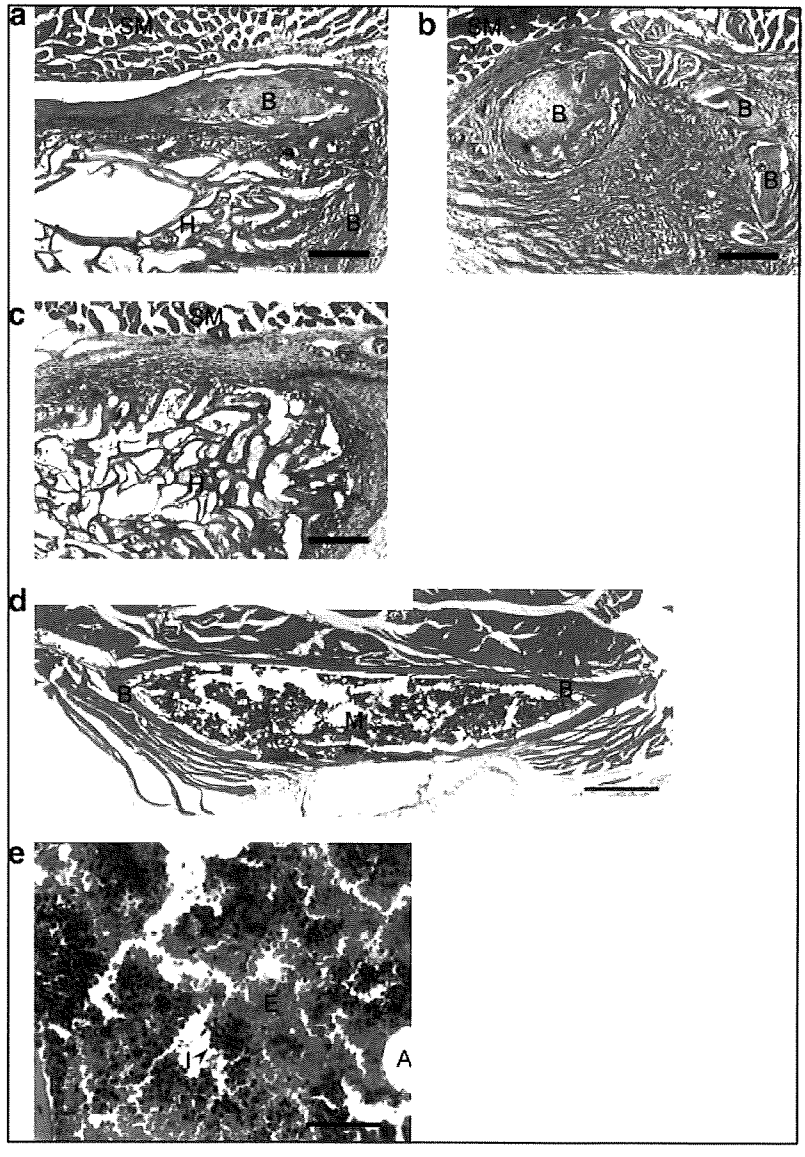

FIG. 3. (**a–c**) Histological image of tissues around the implanted site at 2 weeks after implantation of (**a**) the gelatin hydrogel incorporating BMP-2 (3 μg) with a water content of 97.5 wt%, (**b**) the gelatin hydrogel incorporating BMP-2 (3 μg) with a water content of 99.3 wt%, and (**c**) the gelatin hydrogel incorporating PBS with a water content of 97.5 wt%. B, bone tissue; M, bone marrow-like structure; SM, subcutaneous muscle tissue; H, remaining gelatin hydrogels. (**d**) Histological image of tissues around the implanted site at 7 weeks after implantation of gelatin hydrogel incorporating BMP-2 (3 μg) with a water content of 97.5 wt%. Scale bar = 500 μm. (**e**) Higher magnification image of bone marrow-like structure inside the implanted site. Scale bar = 50 μm. I, inflammatory cells; E, blood cells; A, adipocyte. Color images available online at www.liebertonline.com/ten.

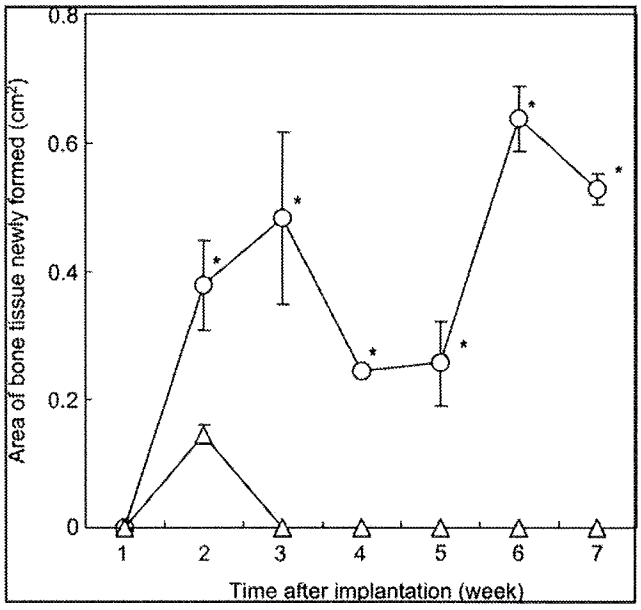

FIG. 4. Area of newly formed bone tissues after implantation of gelatin hydrogels incorporating BMP-2 (3 μg) with a water content of 97.5 wt% (○), gelatin hydrogels incorporating BMP-2 (3 μg) with a water content of 99.3 wt% (Δ). *$p < 0.05$, significant against the area after implantation of gelatin hydrogels incorporating BMP-2 (3 μg) with a water content of 99.3 wt% at the corresponding time.

Recruitment of cells by gelatin hydrogels incorporating BMP-2

Figure 5 shows the fluorescent images of tissues around the implanted site at 2 weeks after the implantation of gelatin hydrogels incorporating BMP-2 or PBS. Irrespective of the experimental groups, a green fluorescence was detected in the implanted sites, which indicates the accumulation of bone marrow-derived cells.

Figure 6 shows the immunofluorescent images of tissues around the implanted site at 2 weeks after implantation of gelatin hydrogels incorporating BMP-2 or PBS. Cells with green fluorescence were observed in all images, and the cells were of round and spindle shape. For the gelatin hydrogels incorporating BMP-2, many red-stained cells were observed around the implanted site (Fig. 6a, b). On the contrary, no cells with red fluorescence were observed around the implanted site of gelatin hydrogels without BMP-2 (Fig. 6c). Figure 7 shows the relative percentage number of GFP-positive cells to osteocalcin-positive cells around the implanted site at 2 weeks after implantation of gelatin hydrogels incorporating BMP-2 or PBS. The implantation of gelatin hydrogels incorporating BMP-2 with different water contents increased the relative percentage number of GFP-positive cells to osteocalcin-positive cells around the implanted site. And the relative percentage for the gelatin hydrogel incorporating BMP-2 with a water content of 97.5 wt% was significantly higher than that of hydrogels with a water content 99.3 wt%. After this time point, it was practically impossible to compare the accumulation of bone marrow-derived cells between the implanted sites of the gelatin hydrogel incorporating BMP-2 with water contents of 97.5 and 99.3 wt%. This is due to the disappearance of the newly formed bone tissue around the implanted site of the latter gelatin hydrogel incorporating BMP-2.

In vitro *cell migration*

Figure 8 shows the number of cells that migrated to the bottom side of the inserts at 24 h after incubation with αMEM containing BMP-2 or other factors. No activity as a chemoattractant to bone marrow cells was observed for BMP-2. The migration level was the same as that of the negative control (0.5 vol% FBS). However, a strong chemoattractant activity was observed for SDF-1 and PlGF, which was the same as that of the positive control (15 vol% FBS). The activity by PlGF was significantly higher than that by SDF-1 and 15 vol% FBS.

Discussion

This study demonstrates that the BMP-2 release profile affected the extent of accumulation of bone marrow-derived cells and the consequent *de novo* generation of bone tissues. The hydrogel water contents of 97.5 and 99.3 wt% indicated that the weight ratio of gelatin molecules to total hydrogel were 2.5 and 0.7 wt%. The difference in gelatin molecule fraction and crosslinking density of hydrogels caused the difference in hydrogel degradation and the consequent BMP-2 *in vivo* release profiles (Fig. 1). The BMP-2 release for a longer time period enabled strong accumulation of GFP-positive bone marrow-derived osteoblast progenitor cells which are also stained with the anti-osteocalcin antibody, even at 2 weeks after implantation. It is apparent from Figure 5 that the accumulation of bone marrow-derived cells was observed by the implantation of gelatin hydrogels with or without BMP-2. However, from the double-staining assay, for the hydrogel without BMP-2, no osteocalcin-positive cells were detected around the implanted site (Figs. 6 and 7). As

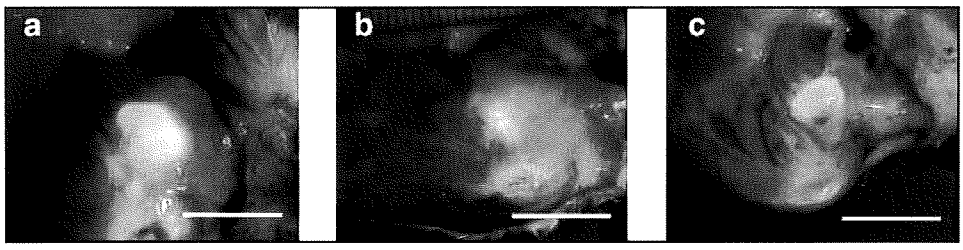

FIG. 5. Fluorescent images of the area surrounding the implant at 2 weeks after implantation of (**a**) the gelatin hydrogel incorporating BMP-2 (3 μg) with a water content of 97.5 wt%, (**b**) the gelatin hydrogel incorporating BMP-2 (3 μg) with a water content of 99.3 wt%, and (**c**) the gelatin hydrogel incorporating PBS with a water content of 97.3 wt%. Scale bar = 1 cm. Color images available online at www.liebertonline.com/ten.

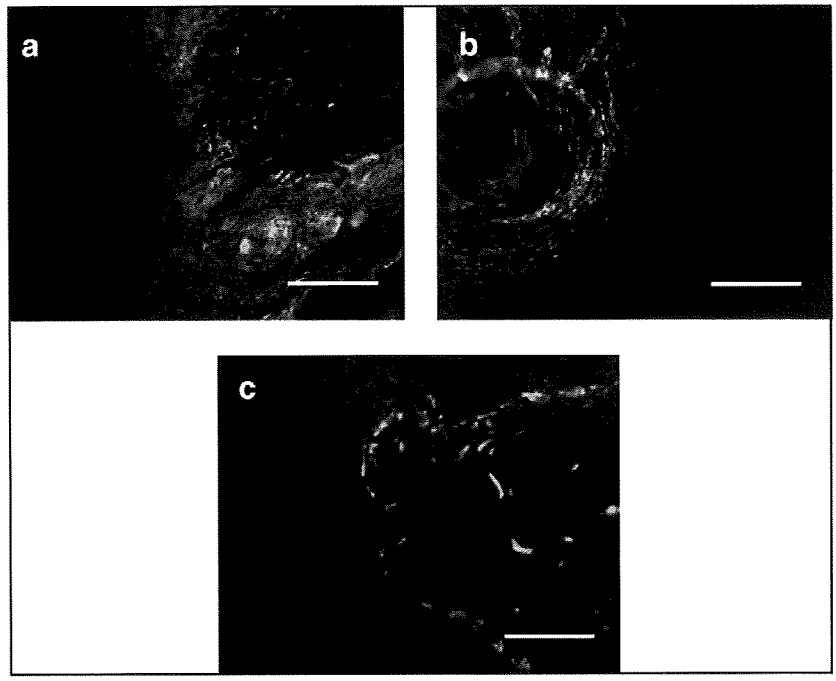

FIG. 6. Immunofluorescence staining images of tissue around the implanted site at 2 weeks after implantation of (a) the gelatin hydrogel incorporating BMP-2 (3 μg) with a water content of 97.5 wt%, (b) the gelatin hydrogel incorporating BMP-2 (3 μg) with a water content of 99.3 wt%, and (c) the gelatin hydrogel incorporating PBS with a water content of 97.3 wt%. Red fluorescence: osteocalcin; green fluorescence: green fluorescent protein. Scale bar = 200 μm. Color images available online at www.liebertonline.com/ten.

the osteocalcin-expressing cells are generally osteoblastic cells with bone formation activity, we can say with certainty that the BMP-2 release increased the recruitment of osteogenic cells around the release site.

The extent of *de novo* generation of bone tissue depended on the water content of gelatin hydrogels. This finding was experimentally confirmed in a previous study[26] and the present results are also in accordance to it even after extended time course (7 weeks after implantation). The decrease in the *de novo* generated area was observed in 4 or 5 and 3 weeks after implantation for gelatin hydrogels with water contents of 97.5 and 99.3 wt%, respectively (Fig. 4). This time profile can be explained in terms of that of BMP-2 release. For the gelatin hydrogel, the time profile of BMP-2 release was well correlated to that of hydrogel degradation. The hydrogel that is degraded for 4–5 weeks would release

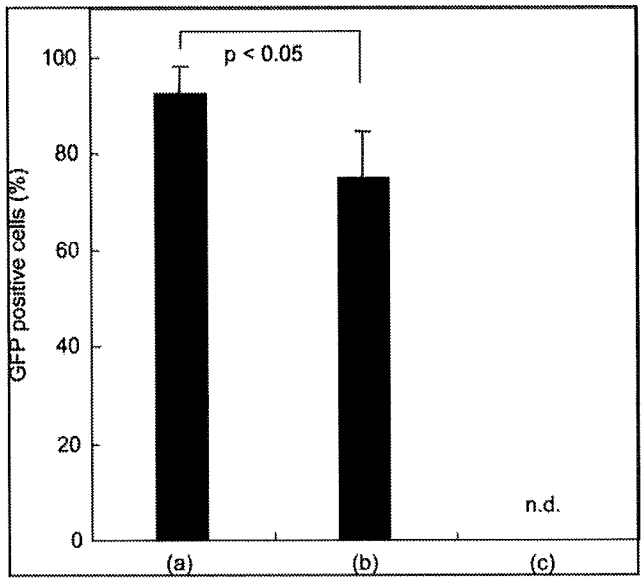

FIG. 7. Relative percentage number of GFP-positive cells to osteocalcin-positive cells around the implanted site at 2 weeks after implantation of (a) gelatin hydrogels incorporating BMP-2 (3 μg) with a water content of 97.5 wt%, (b) gelatin hydrogels incorporating BMP-2 (3 μg) with a water content of 99.3 wt%, and (c) gelatin hydrogels incorporating PBS with a water content of 97.5 wt%. n.d., not detected; GFP, green fluorescent protein.

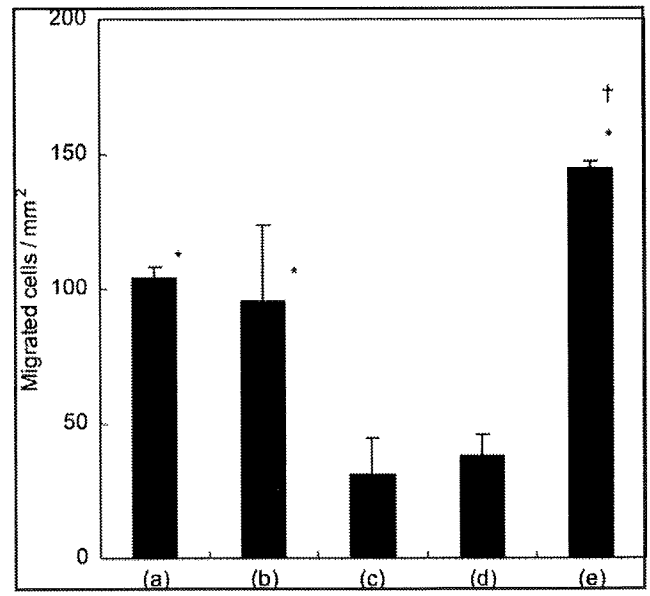

FIG. 8. Migration of bone marrow cells through the transwell membrane at 24 h after incubation with α-minimum essential medium containing (a) 15 vol% fetal bovine serum, (b) 100 ng/mL stromal cell-derived factor-1, (c) 100 ng/mL BMP-2, (d) 0.5 vol% fetal bovine serum, and (e) 100 ng/mL placental growth factor. $^{*}p < 0.05$ against the groups (c) and (d); $^{\dagger}p < 0.05$ significant against the groups (a) and (b).

BMP-2 for 4–5 weeks. It is possible that for this range, the BMP-2 release results in the BMP-induced *de novo* generation of bone tissue. However, the cessation of release would suppress bone tissue induction, resulting in the disappearance of bone tissue. The area of *de novo* generated bone increased again from 6 weeks after implantation. The cells recruited by the released and remaining BMP-2 may be able to further promote *de novo* generation of bone tissue. This reason is not clear at present.

Significant difference in the accumulation of osteocalcin-positive cells between the gelatin hydrogels with water contents of 97.5 and 99.3 wt% was observed (Fig. 6). This experimental result indicates that the profile of BMP-2 release affects the recruitment of bone marrow-derived cells. It is conceivable that BMP-2 release for a longer time period induces the recruitment of cells for a long time period, resulting in enhanced accumulation of cells. BMP-2 can accelerate bone tissue formation[18] through osteoblast migration,[31] by promoting osteogenic differentiation of mesenchymal stem cells,[32,33] angiogenesis,[34] apoptosis of osteoblast,[35] and recruitment of osteoblast progenitor cells.[21,29] It has been demonstrated that BMP-2 could induce the expression of PlGF. The enhanced expression of PlGF promoted the recruitment of progenitor cells from the bone marrow.[36–38] In addition, fibrous tissue and hypertrophic cartilage formation was observed in a fracture healing model of PlGF-deficient mice.[37] The chemoattractant study revealed that PlGF accelerated the migration of isolated bone marrow cells, in contrast to BMP-2 (Fig. 8). It is highly conceivable that BMP-2 functions as a trigger molecule to induce PlGF for the migration of bone marrow-derived cells. Further analysis is needed to understand the effect of BMP-2 release on cell recruitment.

This study clearly indicates that the BMP-2-releasing materials enhance cell accumulation for *de novo* generation of bone tissue. This activity could be modified by the release profile. This finding opens a new strategy of tissue engineering to achieve tissue regeneration by induction of cells present in the body.

Disclosure Statement

No competing financial interests exist.

References

1. Langer, R. Tissue engineering: perspectives, challenges, and future directions. Tissue Eng **13,** 1, 2007.
2. Morrison, S.J., and Spradling, A.C. Stem cells and niches: mechanisms that promote stem cell maintenance throughout life. Cell **132,** 598, 2008.
3. Ingber, D.E., Mow, V.C., Butler, D., Niklason, L., Huard, J., Mao, J., Yannas, I., Kaplan, D., and Vunjak-Novakovic, G. Tissue engineering and developmental biology: going biomimetic. Tissue Eng **12,** 3265, 2006.
4. Matsumoto, T., and Mooney, D.J. Cell instructive polymers. Adv Biochem Eng Biotechnol **102,** 113, 2006.
5. Badylak, S.F. The extracellular matrix as a biologic scaffold material. Biomaterials **28,** 3587, 2007.
6. Ceradini, D.J., Kulkarni, A.R., Callaghan, M.J., Tepper, O.M., Bastidas, N., Kleinman, M.E., Capla, J.M., Galiano, R.D., Levine, J.P., and Gurtner, G.C. Progenitor cell trafficking is regulated by hypoxic gradients through HIF-1 induction of SDF-1. Nat Med **10,** 858, 2004.
7. Eghbali-Fatourechi, G.Z., Lamsam, J., Fraser, D., Nagel, D., Riggs, B.L., and Khosla, S. Circulating osteoblast-lineage cells in humans. N Engl J Med **352,** 1959, 2005.
8. Grunewald, M., Avraham, I., Dor, Y., Bachar-Lustig, E., Itin, A., Yung, S., Chimenti, S., Landsman, L., Abramovitch, R., and Keshet, E. VEGF-induced adult neovascularization: recruitment, retention, and role of accessory cells. Cell **124,** 175, 2006.
9. Jin, D.K., Shido, K., Kopp, H.G., Petit, I., Shmelkov, S.V., Young, L.M., Hooper, A.T., Amano, H., Avecilla, S.T., Heissig, B., Hattori, K., Zhang, F., Hicklin, D.J., Wu, Y., Zhu, Z., Dunn, A., Salari, H., Werb, Z., Hackett, N.R., Crystal, R.G., Lyden, D., and Rafii, S. Cytokine-mediated deployment of SDF-1 induces revascularization through recruitment of $CXCR4^+$ hemangiocytes. Nat Med **12,** 557, 2006.
10. Karp, J.M., and Leng Teo, G.S. Mesenchymal stem cell homing: the devil is in the details. Cell Stem Cell **4,** 206, 2009.
11. Kuznetsov, S.A., Mankani, M.H., Gronthos, S., Satomura, K., Bianco, P., and Robey, P.G. Circulating skeletal stem cells. J Cell Biol **153,** 1133, 2001.
12. Wan, C., He, Q., and Li, G. Allogenic peripheral blood derived mesenchymal stem cells (MSCs) enhance bone regeneration in rabbit ulna critical-sized bone defect model. J Orthop Res **24,** 610, 2006.
13. Wragg, A., Mellad, J.A., Beltran, L.E., Konoplyannikov, M., San, H., Boozer, S., Deans, R.J., Mathur, A., Lederman, R.J., Kovacic, J.C., and Boehm, M. VEGFR1/CXCR4-positive progenitor cells modulate local inflammation and augment tissue perfusion by a SDF-1-dependent mechanism. J Mol Med **86,** 1221, 2008.
14. Zhou, B., Han, Z.C., Poon, M.C., and Pu, W. Mesenchymal stem/stromal cells (MSC) transfected with stromal derived factor 1 (SDF-1) for therapeutic neovascularization: enhancement of cell recruitment and entrapment. Med Hypotheses **68,** 1268, 2007.
15. Zhu, W., Boachie-Adjei, O., Rawlins, B.A., Frenkel, B., Boskey, A.L., Ivashkiv, L.B., and Blobel, C.P. A novel regulatory role for stromal-derived factor-1 signaling in bone morphogenic protein-2 osteogenic differentiation of mesenchymal C2C12 cells. J Biol Chem **282,** 18676, 2007.
16. Tabata, Y. Significance of release technology in tissue engineering. Drug Discov Today **10,** 1639, 2005.
17. Reddi, A.H. Bone morphogenetic proteins: from basic science to clinical applications. J Bone Joint Surg Am **83-A Suppl 1,** S1, 2001.
18. Wozney, J.M. Overview of bone morphogenetic proteins. Spine **27,** S2, 2002.
19. Wozney, J.M., Rosen, V., Celeste, A.J., Mitsock, L.M., Whitters, M.J., Kriz, R.W., Hewick, R.M., and Wang, E.A. Novel regulators of bone formation: molecular clones and activities. Science **242,** 1528, 1988.
20. Bessa, P.C., Casal, M., and Reis, R.L. Bone morphogenetic proteins in tissue engineering: the road from laboratory to clinic, part II (BMP delivery). J Tissue Eng Regen Med **2,** 81, 2008.
21. Otsuru, S., Tamai, K., Yamazaki, T., Yoshikawa, H., and Kaneda, Y. Bone marrow-derived osteoblast progenitor cells in circulating blood contribute to ectopic bone formation in mice. Biochem Biophys Res Commun **354,** 453, 2007.
22. Bruder, S.P., Fink, D.J., and Caplan, A.I. Mesenchymal stem cells in bone development, bone repair, and skeletal regeneration therapy. J Cell Biochem **56,** 283, 1994.
23. Colnot, C., Huang, S., and Helms, J. Analyzing the cellular contribution of bone marrow to fracture healing using bone marrow transplantation in mice. Biochem Biophys Res Commun **350,** 557, 2006.